0 0 0 0 2 2 0 2 4 3 8

UCRL-11510

University of California

Ernest O. Lawrence Radiation Laboratory

PROPERTIES OF THE NEUTRAL CASCADE HYPERON

[redacted]

(Bldg. 50)

[redacted]

Berkeley, California

DISCLAIMER

This document was prepared as an account of work sponsored by the United States Government. While this document is believed to contain correct information, neither the United States Government nor any agency thereof, nor the Regents of the University of California, nor any of their employees, makes any warranty, express or implied, or assumes any legal responsibility for the accuracy, completeness, or usefulness of any information, apparatus, product, or process disclosed, or represents that its use would not infringe privately owned rights. Reference herein to any specific commercial product, process, or service by its trade name, trademark, manufacturer, or otherwise, does not necessarily constitute or imply its endorsement, recommendation, or favoring by the United States Government or any agency thereof, or the Regents of the University of California. The views and opinions of authors expressed herein do not necessarily state or reflect those of the United States Government or any agency thereof or the Regents of the University of California.

0 0 0 0 2 2 0 2 5 0 0

Special Thesis

UCRL-11510

UNIVERSITY OF CALIFORNIA
Lawrence Radiation Laboratory
Berkeley, California

AEC Contract No. W-7405-eng-48

PROPERTIES OF THE NEUTRAL CASCADE HYPERON

John Richard Hubbard
(Ph.D. Thesis)

April 25, 1966

0 0 0 0 2 2 0 2 6 5 8

PROPERTIES OF THE NEUTRAL CASCADE HYPERON

Contents

Abstract v

I. Introduction 1

II. Analysis of Events

A. Beam System 2

B. General Analysis

1. Topological Scanning 2

2. Kinematic Fitting 4

3. Ambiguity Rate 8

C. The 2V0p Topology

1. Reaction Channels 9

2. Short Neutral Tracks 9

D. The 1V2p Topology 13

III. Production Analysis

A. Pathlength 16

B. Cross Sections 16

C. Exchange Mechanisms

1. Crossing Matrices 21

2. Single-Particle Exchanges 23

D. SU(n) Symmetry 24

IV. Decay Asymmetry

A. Theory 28

B. Results 30

V. Lifetime

A. Restrictions on Sample 32

B. Calculation of Ξ^0 Length 32

C. Likelihood Formulation 33

D. Results 35

VI. Rare Decay Modes

A. Dalitz Events 37

B. Other Ξ^0 Decay Modes 39

1. Theory 39

2. Results 42

Acknowledgments 45

Appendix: Lifetime Likelihood Formulation 46

1. Lifetime from the Ξ^0 Length 46

2. Lifetime from the Link Joining the Ξ^0 Production and Λ Decay Vertices 48

Footnotes and References 50

0 0 0 0 2 3 0 3 8 8 p

PROPERTIES OF THE NEUTRAL CASCADE HYPERON

John Richard Hubbard

Lawrence Radiation Laboratory
University of California
Berkeley, California

April 25, 1966

ABSTRACT

The production of neutral cascade hyperons by incident K^- on hydrogen has been studied from threshold at 1.05 BeV/c to 1.7 BeV/c. A sample of 206 Ξ^0 events was obtained. Production cross sections rise to about 120 μb for Ξ^0K^0, 25 μb for $\Xi^0K^0\pi^0$, and 50 μb for $\Xi^0K^+\pi^-$ at 1.7 BeV/c. The mean life is $\tau_{\Xi^0} = 2.53^{+0.28}_{-0.23} \times 10^{-10}$ sec. The decay asymmetry is $\alpha_{\Xi^0} = -0.20 \pm 0.22$. The branching ratios are less than 1% for $\Xi^0 \rightarrow \Sigma^{\pm}\ell^{\mp}\nu$, $\Xi^0 \rightarrow p\ell^-\nu$, and $\Xi^0 \rightarrow p\pi^-$, where $\ell^{\pm}$ signifies $e^{\pm}$ or $\mu^{\pm}$.

I. INTRODUCTION

The negative cascade hyperon was first observed in 1952.[1] The strangeness scheme of Gell-Mann and Nishijima accommodates the cascade as an I-spin doublet and requires the existence of a neutral cascade (Ξ^0).[2] The Ξ^0 was first identified experimentally in 1959.[3]

In the present experiment, 206 Ξ^0 hyperons were observed when the Lawrence Radiation Laboratory's 72-in. bubble chamber was exposed to a separated beam of K^- mesons. The incident momentum was varied from 1.0 to 1.7 BeV/c. The published Ξ^- and Ξ^0 results for this experiment require no substantial modification.[4-7] The Ξ^0K^0 cross section rises from threshold at 1.05 BeV/c to about 120 μb at 1.7 BeV/c. The threshold for the three-body production modes is 1.38 BeV/c; the cross sections rise sharply from the $\Xi^*(1530)$ threshold at 1.49 BeV/c to about 25 μb for $\Xi^0K^0\pi^0$ and 50 μb for $\Xi^0K^+\pi^-$ at 1.7 BeV/c.

The $|\Delta I| = 1/2$ rule for nonleptonic weak decays[8] requires $A_{\Xi^0} = -A_{\Xi^-}/\sqrt{2}$, where A_Ξ is the amplitude for the decay $\Xi \to \Lambda + \pi$. We compare our Ξ^0 results with the Ξ^- results from the same experiment.[4-6] The decay asymmetries yield $\alpha_{\Xi^0}/\alpha_{\Xi^-} = 0.5 \pm 0.6$, consistent with the prediction of equality. The decay rates yield $\lambda_{\Xi^0}/\lambda_{\Xi^-} = 0.67 \pm 0.08$, two standard deviations from the prediction of 0.5.

We searched for new Ξ^0 decay modes: $\Xi^0 \to \Sigma^\pm \ell^\mp \nu$, $\Xi^0 \to p\ell^-\nu$, and $\Xi^0 \to p\pi^-$, where $\ell^\pm$ denotes a charged lepton. No definite examples were found. The branching ratios for these decay modes are less than 1%.

II. ANALYSIS OF EVENTS

A. Beam System

The K^- were separated from the π^- in two stages by 20-ft-long, 500 kV, glass-cathode velocity spectrometers.[9] A schematic of the beam-transport system is shown in Fig. 1.[10]

B. General Analysis

1. Topological Scanning

We studied the following Ξ^0 production reactions:

$$K^- + p \rightarrow \Xi^0 + K^0, \qquad 146 \text{ events;}$$

$$K^- + p \rightarrow \Xi^0 + K^0 + \pi^0, \qquad 8 \text{ events;}$$

$$K^- + p \rightarrow \Xi^0 + K^+ + \pi^-, \qquad 52 \text{ events.}$$

Berge et al. analyzed 1004 Ξ^- events from the same experiment.[4] We require a visible two-body decay for each Λ and K^0. The complete reactions studied are:

$$K^- + p \rightarrow \underbrace{\Xi^0}_{\underbrace{\Lambda + \pi^0}_{\underbrace{p + \pi^-}}} + \underbrace{K^0}_{\pi^+ + \pi^-} \tag{2.1}$$

$$K^- + p \rightarrow \underbrace{\Xi^0}_{\underbrace{\Lambda + \pi^0}_{\underbrace{p + \pi^-}}} + \underbrace{K^0}_{\pi^+ + \pi^-} + \pi^0 \tag{2.2}$$

$$K^- + p \rightarrow \underbrace{\Xi^0}_{\underbrace{\Lambda + \pi^0}_{\underbrace{p + \pi^-}}} + K^+ + \pi^- \tag{2.3}$$

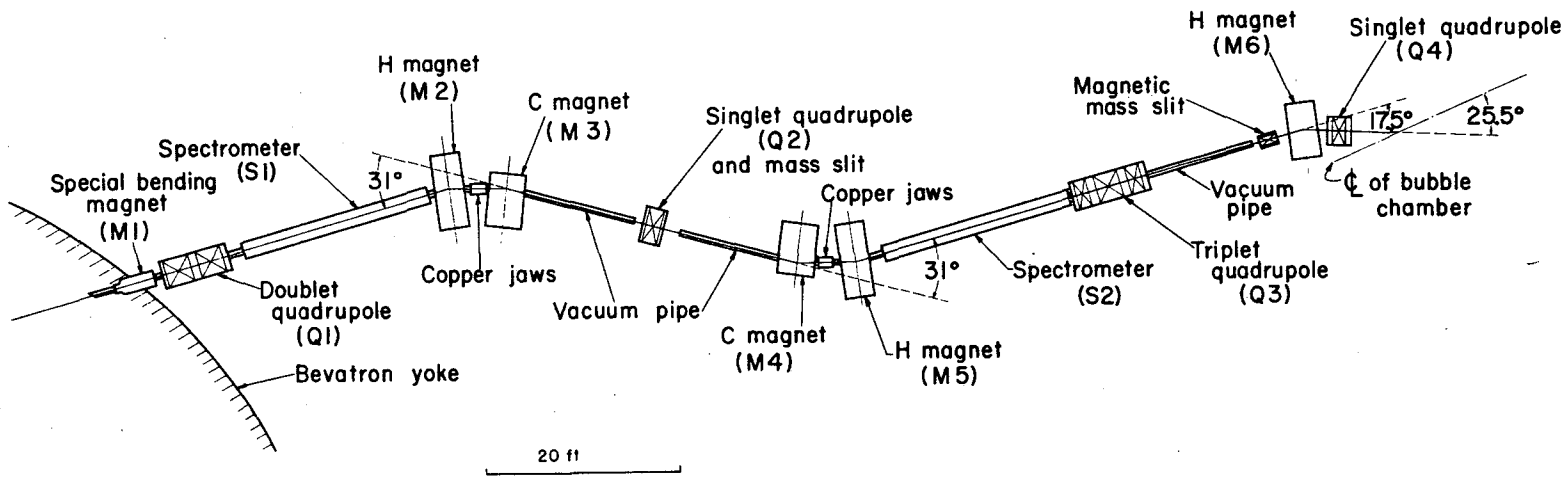

Fig. 1. Beam-transport system.

The topologies of interest are thus the 2V0p (two-Vee, zero-prong) for (2.1) and (2.2), and 1V2p (one-Vee, two-prong) for (2.3). These topologies are shown in Figs. 2 and 3.

All film was scanned at least twice.[11] The nominal single-scan efficiencies were 90% for 2V0p events and 96% for 1V2p events. The overall scan efficiencies were thus about 99%. Systematic effects that upset this result will be discussed for each topology.

2. Kinematic Fitting

A schematic diagram of the $\Xi^0 K^0$ production and decay chain of (2.1) is given in Fig. 4. The production point is uncertain within about one mean bubble gap; therefore, the beam track has been extended by (0.05 ± 0.05) cm. Our kinematic fitting tests the consistency of each hypothesis with conservation of energy and momentum. If no information is missing, conservation of energy and the three momentum components provide four conditions, or "constraints," at each production or decay vertex. The $\Xi^0 K^0$ reaction is analyzed as follows: First the Λ and K^0 decays are fit kinematically. The line of flight of the Λ, as well as the momenta of the neutral tracks, is unknown, leaving only one constraint for the Λ, but three for the K^0. Then the Ξ^0 production and decay vertices are constrained simultaneously. There are three constraints in this final fit; in addition to two kinematic constraints, there is a geometric condition that the Λ line of flight intersect the Ξ^0 line of flight in space. This geometric condition is equivalent to the requirement that the Ξ^0 and Λ momentum vectors and X, the "link" from the production vertex to the Λ decay point, be coplanar.[12]

The Ξ^0 length, ℓ_{Ξ^0}, is calculated from the measured length of the link, ℓ_X, and the fitted angles. From Fig. 4, we have

$$\ell_{\Xi^0} = \ell_X \sin\alpha_2 / \sin\theta, \tag{2.4}$$

where θ is the Ξ^0 decay angle in the laboratory, and α_2 is the angle between the Λ and the link. This calculated Ξ^0 length can be negative, because the fitted Λ line of flight can intersect the Ξ^0 line of flight before, rather than after, the production point. The uncertainty in the calculated length is typically about 20%.

0 0 0 0 2 2 0 2 6 0 4

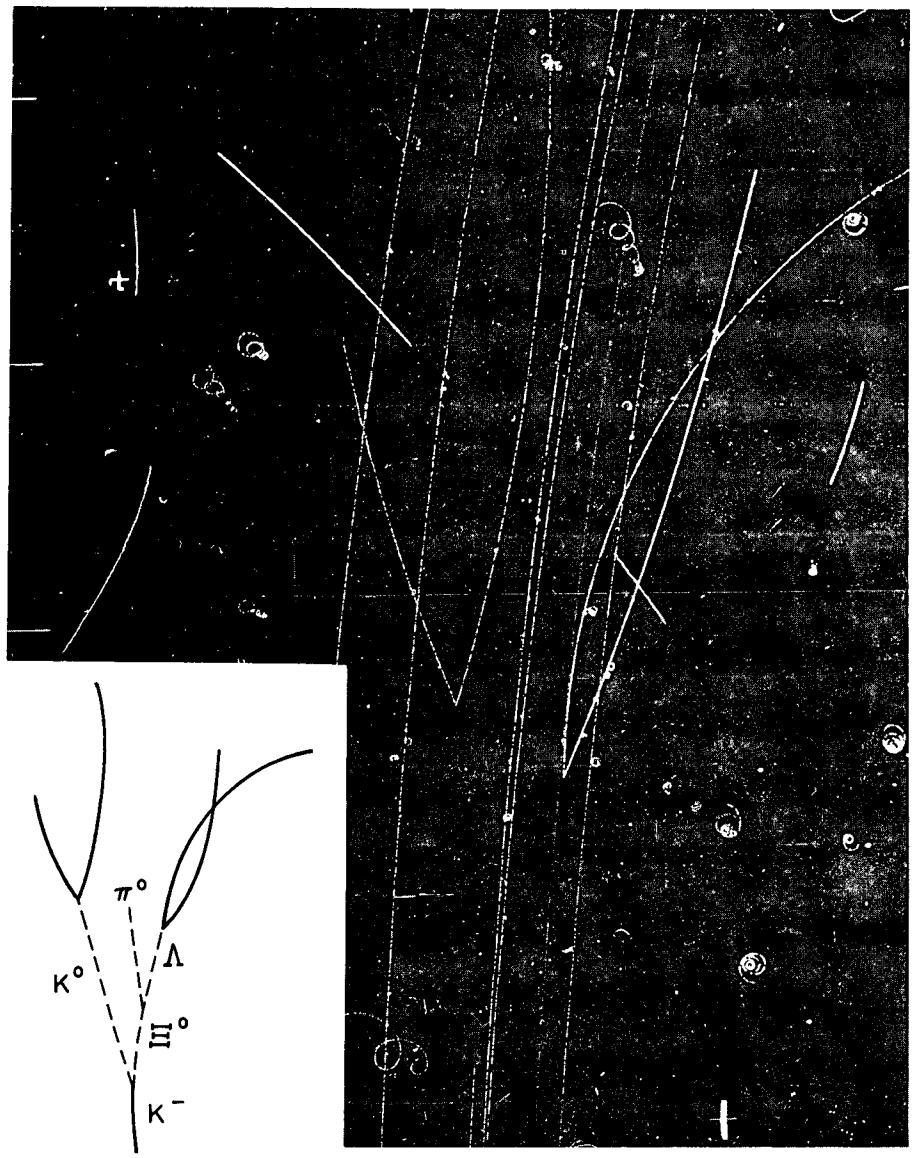

ZN-5482

Fig. 2. 2V0p topology: $\Xi^0 K^0$ production.

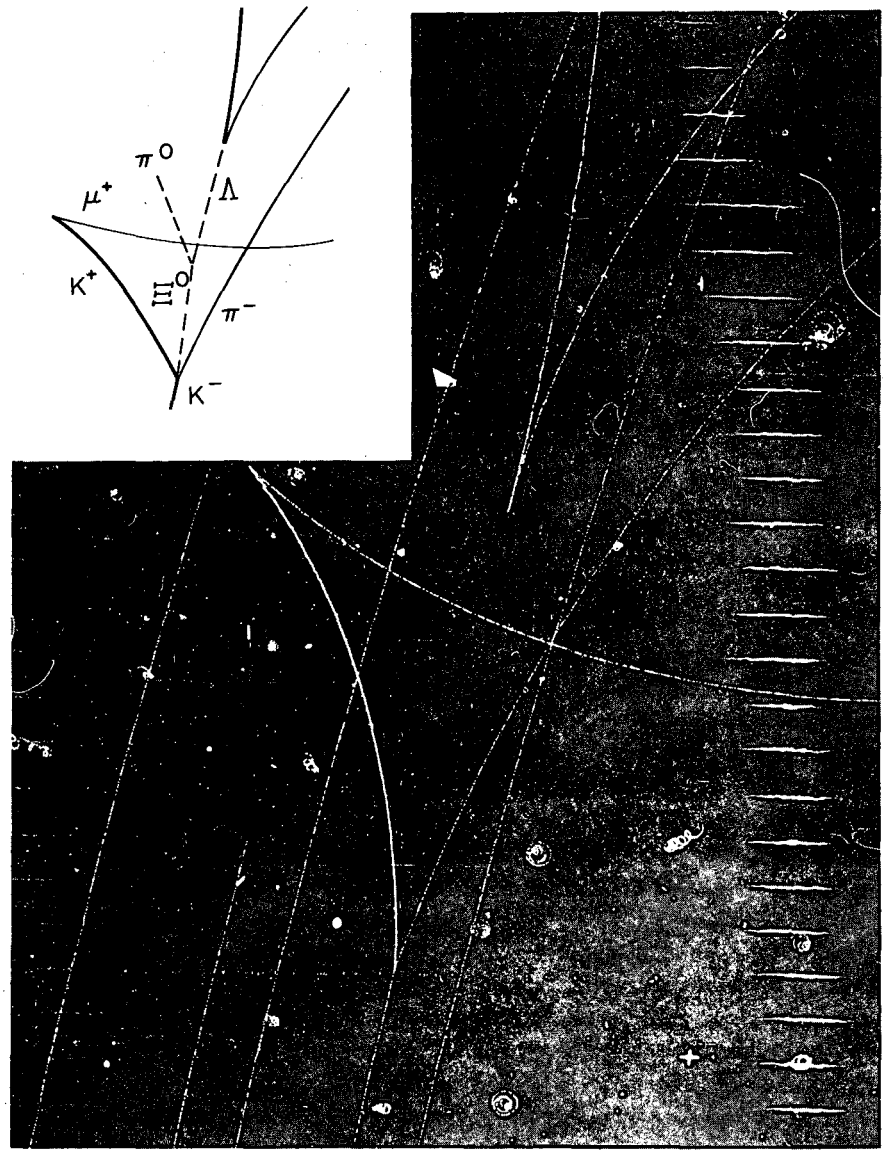

ZN-5481

Fig. 3. 1V2p topology: $\Xi^0 K^+ \pi^-$ production.

0 0 0 0 2 3 0 3 5 6 3

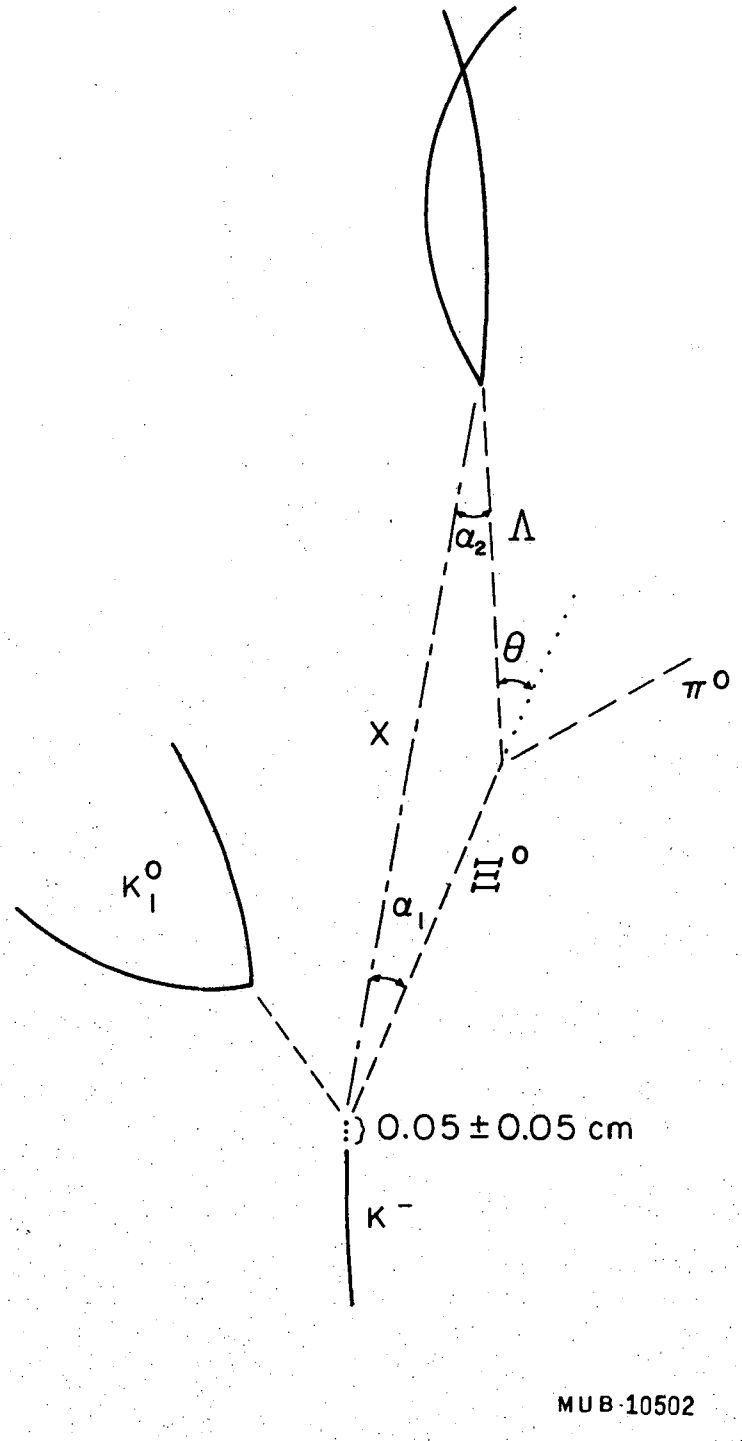

Fig. 4. Schematic of $\Xi^0 K^0$ production and decay. X is the "link" from the production vertex to the Λ decay. The beam track has been extended by one mean bubble gap.

3. Ambiguity Rate

Ambiguities between Ξ^0 production modes and Λ and Σ^0 production modes of the same topologies can distort our results. For Λ and Σ^0 production modes, the Λ must come directly from the primary vertex. Therefore, these ambiguities occur only if the Λ direction coincides with the link direction; experimentally, α_2/σ_α must be small, where σ_α is the uncertainty in α_2. Knowledge of the form of α_2/σ_α helps us eliminate systematic errors.

For a Ξ^0 event, we obtain α_2 from (2.4), in terms of the laboratory decay angle, θ. Transforming the Ξ^0 decay from the rest frame, we obtain

$$\tan\theta = \frac{M_\Xi q_\Lambda \sin\theta^*}{E_\Xi q_\Lambda \cos\theta^* + p_\Xi \epsilon_\Lambda}, \tag{2.5}$$

where θ^* is the Λ angle in the Ξ rest frame with respect to the Ξ direction in the laboratory system, $(\epsilon_\Lambda, q_\Lambda)$ is the Λ energy-momentum in the Ξ rest frame, with $q_\Lambda = 135$ MeV/c, and (E_Ξ, p_Ξ) is the Ξ^0 energy-momentum in the laboratory. For our beam momenta, $p_{\Xi^0} > 500$ MeV/c, and (2.5) requires $\theta < 20$ deg. From (2.4) and (2.5), the principal dependence of α_2 is

$$\alpha_2 \sim t_{\Xi^0} \sin\theta^*/\ell_X, \tag{2.6}$$

where $t_{\Xi^0} = M_\Xi \ell_\Xi / p_\Xi$ is the Ξ^0 proper time of flight.

The kinematic fitting of the Λ and the measurement of the link determine the uncertainty, σ_α. The uncertainty from the Λ kinematics varies inversely with p_Λ, the Λ momentum in the laboratory system. The uncertainty from the measured link is inversely proportional to its length. Noting that both p_Λ and ℓ_X vary directly with p_{Ξ^0}, we obtain

$$\alpha_2/\sigma_\alpha \sim t_{\Xi^0} \sin\theta^*, \tag{2.7}$$

roughly independent of p_{Ξ^0}. Thus, ambiguous interpretations are preferentially associated with short Ξ^0 proper times and small $|\sin\theta^*|$.

C. The 2V0p Topology

1. Reaction Channels

In a hydrogen bubble chamber with incident K^-, the 2V0p topology is unambiguously due to Ξ^0 production at our beam momenta.[13] There is π^- contamination in the beam, however. A list of possible 2V0p events includes:

$$K^- + p \rightarrow \Xi^0 + K^0, \qquad \Xi^0 \rightarrow \Lambda + \pi^0 \qquad [3C] \qquad (2.1)$$

$$K^- + p \rightarrow \Xi^0 + K^0 + \pi^0, \qquad \Xi^0 \rightarrow \Lambda + \pi^0 \qquad [0C] \qquad (2.2)$$

$$\pi^- + p \rightarrow \Lambda + K^0 \qquad [4C] \qquad (2.8)$$

$$\pi^- + p \rightarrow \Sigma^0 + K^0, \qquad \Sigma^0 \rightarrow \Lambda + \gamma \qquad [2C] \qquad (2.9)$$

$$\pi^- + p \rightarrow \Lambda + K^0 + \pi^0, \qquad [1C] \qquad (2.10)$$

where [0C], [1C], etc. is the number of constraints in the reaction. For the π^- production modes, the Λ decay has three constraints, rather than one, because the Λ direction must coincide with the measured link.

We have analyzed 221 events of the 2V0p topology. Table I presents the set of consistent interpretations and the final apportionment. The number of entries in the table exceeds the number of events, because some events are consistent with three hypotheses. Table II lists the number of events for each channel and the π^- cross sections. The π^- contamination was calculated from the four-constraint $\pi^- p \rightarrow \Lambda K^0$ events, which are nearly unambiguous. The reported π^- cross sections[14] provide a consistency check on the apportionment of ambiguities; our results are consistent, as seen by comparing the last two rows in Table II.

2. Short Neutral Tracks

Events with short neutral tracks can be systematically lost. For the link a cutoff has been imposed at 0.5 cm. This cutoff eliminates seven of the 221 2V0p events, including two events consistent with $\Xi^0 K^0$ production. A posteriori, we expect less than 1% of the Ξ^0 events to fail this criterion (see section V).

Table I. Apportionment of 2V0p events. All consistent interpretations are shown. Three of the events are consistent with three different hypotheses.

Final state	K^- production		π^- production				Final apportionment
	Ξ^0K^0	$\Xi^0K^0\pi^0$	ΛK^0	$\Lambda K^0\pi^0$	Σ^0K^0	$\Sigma^0K^0\pi^0$	
Ξ^0K^0	134		2	4	22		146
$\Xi^0K^0\pi^0$		6		2		1	8
ΛK^0	2		37	1			39
$\Lambda K^0\pi^0$	4	2	1	5	3		8
Σ^0K^0	22			3	10		20
$\Sigma^0K^0\pi^0$		1					0
						Total =	221

The loss of short K^0's is more common. For Ξ^0K^0 production by 1.32-BeV/c incident K^-, a K_1^0 produced backward in the c.m. is at rest in the laboratory, whereas a K_1^0 produced forward in the c.m. has a mean length of 4.25 cm. Figure 5 shows the kinematic limits in the laboratory for K^0's from Ξ^0K^0 and $\Xi^0K^0\pi^0$ production at 1.5-BeV/c incident beam momentum. An absolute length cutoff for the K_1^0 makes cross-section determinations difficult, because we have no a priori knowledge of the production angular distributions.

A Ξ^0K^0 event with a very short K_1^0 appears to have the 1V2p topology. The event will fit $K^-p \rightarrow \Lambda\pi^+\pi^-\pi^0$ if the three-constraint Λ decay fits, with the Λ constrained to come directly from the primary vertex. For about 40% of our Ξ^0K^0 events, the Λ does fit to the primary vertex; this rate is roughly independent of p_{Ξ^0}, as expected from (2.7). Analysis of the 1V2p events in which this three-constraint Λ-decay fit fails can recover the remaining 60% of the missing events. This procedure was used only for events with K^0 momenta below 100 MeV/c; eleven new events were found, indicating (11/0.6) = 18 of these

Table II. Numbers of 2V0p events and π^- contamination. The π^- cross sections are from Schwartz, Ref. 14. The number of events assigned to Σ^0K^0 and $Y^0K^0\pi^0$ [a] is consistent with the expected number. The final column gives the π^- contamination as a percentage of the K^- flux.

P_{beam} (BeV/c)	Ξ^0K^0	$\Xi^0K^0\pi^0$	$\pi^-p \to \Lambda K^0$ N	$\pi^-p \to \Lambda K^0$ $\sigma(\mu b)$	$\pi^-p \to \Sigma^0K^0$ N	$\pi^-p \to \Sigma^0K^0$ $\sigma(\mu b)$	$\pi^-p \to Y^0K^0\pi^0$ [a] N	$\pi^-p \to Y^0K^0\pi^0$ [a] $\sigma(\mu b)$	π^- contamination [b] (N/mb)	π^- contamination [b] (%)
1.05, 1.11	2		2	700	2	350			13 ± 9	5
1.22	7		12	460	6	200			115 ± 35	10
1.33	10		2	340	2	150	1	15	26 ± 19	2
1.43	4		2	335	0	160	1	30	26 ± 19	3.5
1.51	87	1	13	330	7	160	1	50	173 ± 48	3.5
1.60	13	3	1	250	1	120	1	65	18 ± 18	2.5
1.70	23	4	7	200	2	120	4	80	134 ± 57	12.5
Totals										
Observed	146	8	39		20		8			
Expected [b]			input		19.1		5.3			

a. $\Lambda K^0\pi^0 + \Sigma^0K^0\pi^0$. b. Based on observed ΛK^0 events and published cross sections from Ref. 14.

0 0 0 0 2 3 0 5 6 8 7 4

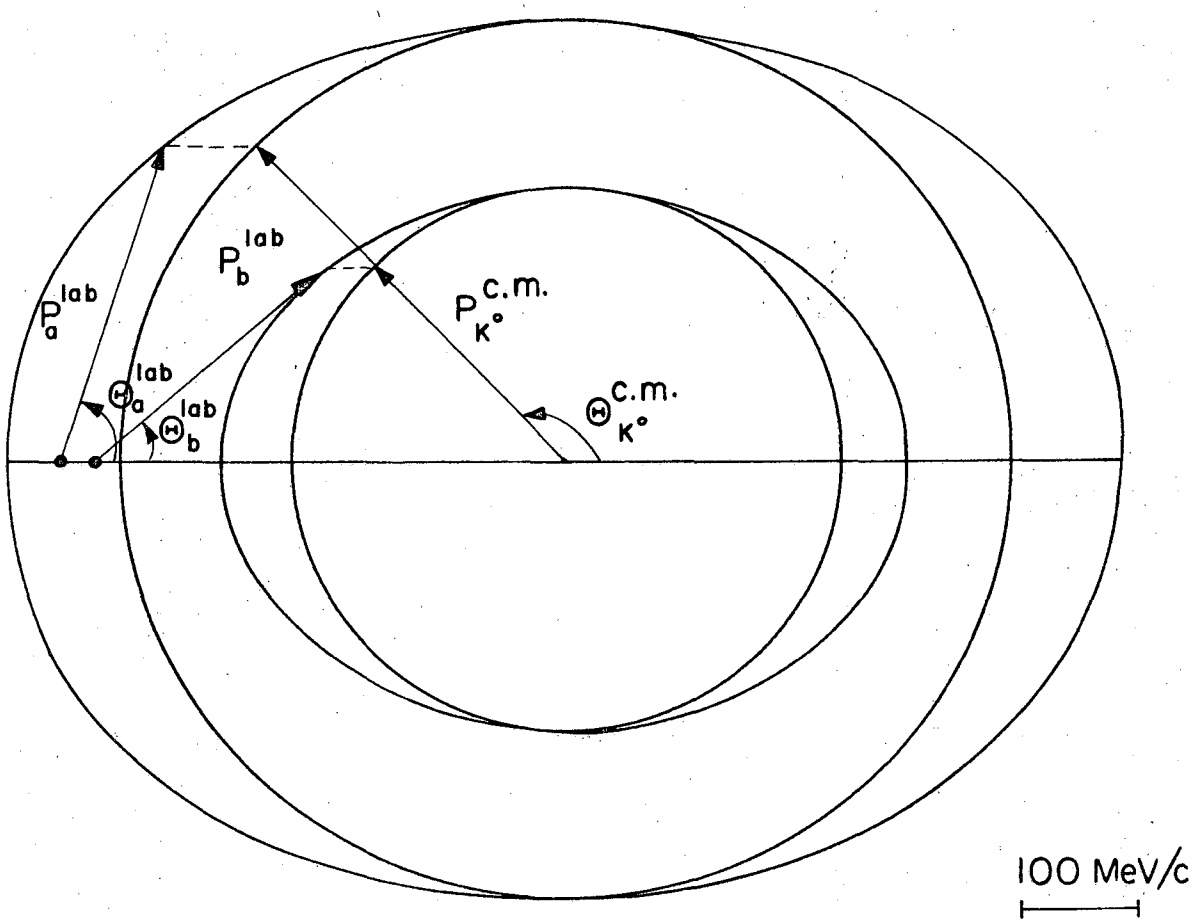

MUB-10500

Fig. 5. K^0 kinematic limits (a) Ξ^0K^0 production. The laboratory momentum vector must lie on the outer ellipse. The minimum K^0 momentum is 45 MeV/c, backward in the laboratory system. (b) $\Xi^0K^0\pi^0$ production. The momentum vector may lie anywhere within the inner ellipse. The minimum K^0 momentum is 105 MeV/c, forward in the laboratory system.

0 0 0 0 2 2 0 2 6 8 9

events missed on the topological scan. Our sample of 146 Ξ^0K^0 events does not include these new events, but the cross-section analysis of section III includes them as a correction. For K^0 momenta above 100 MeV/c, we estimate a loss rate of 5% from short K^0's.

D. The 1V2p Topology

In contrast to the 2V0p topology, the 1V2p topology results from K^- reactions, such as $K^-p \rightarrow \Lambda\pi^+\pi^-$, which are much more copious than Ξ^0 production. Huwe analyzed the 1V2p events with a Λ and obtained good measurements and fit information on about 90% of the events.[15] Wojcicki et al. analyzed the 1V2p events with a K^0.[16] There are 35 000 1V2p events above the $\Xi K\pi$ threshold at 1.38 BeV/c. We gleaned our $\Xi^0K^+\pi^-$ sample from the 7500 events which failed to fit the more common 1V2p reactions in Table III on one measurement. Sixty-one events are consistent with $\Xi^0K^+\pi^-$ production. Table IV shows the final apportionment, in which 52 of these 61 events are accepted in our final sample.[17]

Table III. Common 1V2p production modes. Column 3 contains the acceptable χ^2 level. Column 4 contains the cross section at 1.5 BeV/c, from Refs. 15 and 16.

Final state	Constraints	Maximum χ^2	σ(mb)
$\Lambda\pi^+\pi^-$	4	10.0	2.1
$\Sigma^0\pi^+\pi^-$	2	5.0	0.8
$\Lambda\pi^+\pi^-\pi^0$	1	2.5	2.5
$\bar{K}^0p\pi^-$	4	10.0	1.7
$\bar{K}^0p\pi^-\pi^0$	1	2.5	0.6
$\bar{K}^0\pi^+\pi^-n$	1	2.5	1.0

Table IV. $\Xi^0K^+\pi^-$ sample. The 61 events in the first row fit $\Xi^0K^+\pi^-$; 43 are unambiguous. The second row gives the final apportionment of these events.

Final state	K^- production					π^- production		
	$\Xi^0K^+\pi^-$	$\Lambda\pi^+\pi^-$	$\Lambda\pi^+\pi^-\pi^0$	$\Lambda\pi^+\pi^-\pi^0\pi^0$	$\Sigma^0\pi^+\pi^-$	$\Lambda K^+\pi^-$	$\Lambda K^+\pi^-\pi^0$	$\Sigma^0K^+\pi^-$
$\Xi^0K^+\pi^-$	43	0	8	2	0	1	5	2
Final apportionment	52	0	6	0	0	1	1	1

Systematic effects are certainly present in the above analysis. We lose events that are highly ambiguous with the K^- production modes in Table III. According to Table IV, most of these ambiguities involve $K^-p \rightarrow \Lambda\pi^+\pi^-\pi^0$. Assuming a flat χ^2 distribution for the wrong hypothesis, we conclude that 5% of our events fit $\Lambda\pi^+\pi^-\pi^0$ production and were lost. The final efficiency for recovery of $\Xi^0K^+\pi^-$ events is 85%.

III. PRODUCTION ANALYSIS

A. Pathlength

The total K^- flux at each momentum was determined[18] (1) from the three-prong decays and the published K^- branching ratios[19] and (2) from the sum of all interactions and the published K^- total cross sections.[20]

In the first method, we simply count the three-prong events and divide by the proper K^- decay rate. The three-prong events are either τ-decays, $K^- \rightarrow \pi^-\pi^-\pi^+$, or one-prong decays with an electron pair from a π^0 Dalitz decay, $\pi^0 \rightarrow \gamma e^+e^-$. The total branching ratio is $(5.91 \pm 0.08)\%$.[19]

In the second method, we start with the total number of incident tracks. The π^- contamination is calculated from the observed $\pi^-p \rightarrow \Lambda K^0$ events, with the results already presented in Table II. The e^- and μ^- contamination does not interact strongly. The total number of visible primary interactions was determined and corrected for unseen forward elastic scatters. The K^- and π^- flux account for these interactions; any remaining flux is e^- or μ^- contamination. The K^- pathlength and the contamination are listed in Table V, with the K^- and π^- total cross sections used in the calculation.[20, 21]

The best-estimate pathlength in the final column of Table V is the unweighted mean of the two independent results. This best-estimate value is used in the following analysis.

B. Cross Sections

Numbers of events and total cross sections for the two and three-body Ξ^0 production modes are presented in Table VI and Fig. 6. The uncertainties in the apportionment of ambiguities and in the corrections for systematic effects discussed in section II have been included with our statistical uncertainty.

The differential cross section for Ξ^0K^0 production at 1.5 BeV/c is presented in Fig. 7a. There are peaks in both the forward and backward directions. These qualitative features are independent of variations to include or exclude ambiguous events. For comparison, the

Table V. Total K^- pathlength. The cross sections for K^-p are from Cook et al., Ref. 20; for π^-p, from Diddens et al., Ref. 21. The π^- contamination is from Table II. Section III describes the pathlength determinations in columns 6 and 7; the final column contains the unweighted mean of these two values.

P_{beam} (BeV/c)	$\sigma^{tot}_{K^-p}$ (mb)	$\sigma^{tot}_{\pi^-p}$ (mb)	Contamination (%)		Events /mb		
			π^-	e^-, μ^-	Three-prong decays	Interactions	Best estimate
1.05, 1.11					260 ± 25		260 ± 25
1.22	34.2	36.0	10 ± 3	7 ± 5	1190 ± 50	1300 ± 65	1245 ± 60
1.33	32.4	35.2	2 ± 1.5	5.5 ± 5	1510 ± 60	1410 ± 70	1460 ± 70
1.43	32.3	34.8	3.5 ± 2.5	3 ± 5	820 ± 40	850 ± 40	835 ± 40
1.51	32.5	34.4	3.5 ± 1	0 ± 5	5220 ± 185	5100 ± 200	5160 ± 200
1.60	32.5	34.4	2.5 ± 2.5	1 ± 5	690 ± 35	760 ± 40	725 ± 35
1.70	32.5	34.5	12.5 ± 5	0 ± 5	1090 ± 50	1135 ± 55	1113 ± 55

0 0 0 0 2 3 0 2 5 6 0

Table VI. Numbers of events and channel cross sections. Cross sections have been corrected for scanning efficiency, escape loss, and unseen Λ and K^0 decays. Threshold for ΞK production is 1.05 BeV/c, for $\Xi K\pi$ production, 1.38 BeV/c.

P_{beam} (BeV/c)	$\epsilon_{c.m.}$ (BeV)	N/μb	Ξ^0K^0		$\Xi^0K^0\pi^0$		$\Xi^0K^+\pi^-$	
			N	σ(μb)	N	σ(μb)	N	σ(μb)
1.05, 1.11	1.815	0.26	2	46 ± 35				
1.22	1.896	1.245	7	32 ± 14				
1.33	1.946	1.460	10	43 ± 19				
1.43	1.991	0.835	4	44 ± 20				
1.51	2.028	5.160	87	87 ± 11	1	1 ± 1	15	5 ± 2
1.60	2.066	0.725	13	102 ± 31	3	23 ± 14	10	25 ± 9
1.70	2.109	1.113	23	122 ± 28	4	22 ± 13	27	45 ± 11
	Total:		146		8		52	
	Grand total:				206 Ξ^0 events			

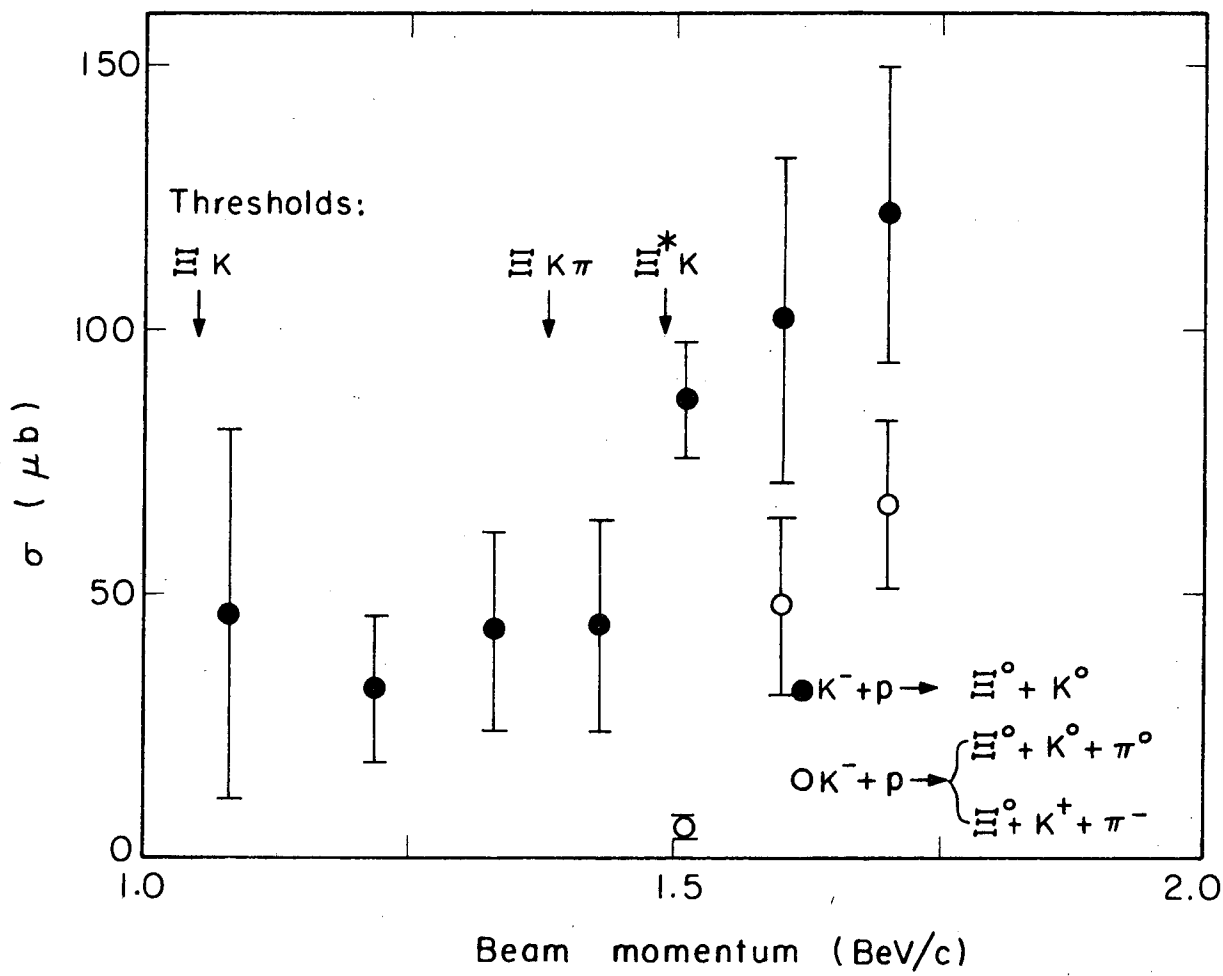

MUB-10506

Fig. 6. Two-body and three-body Ξ^0 production cross sections. Closed circles represent two-body data; open circles, three-body.

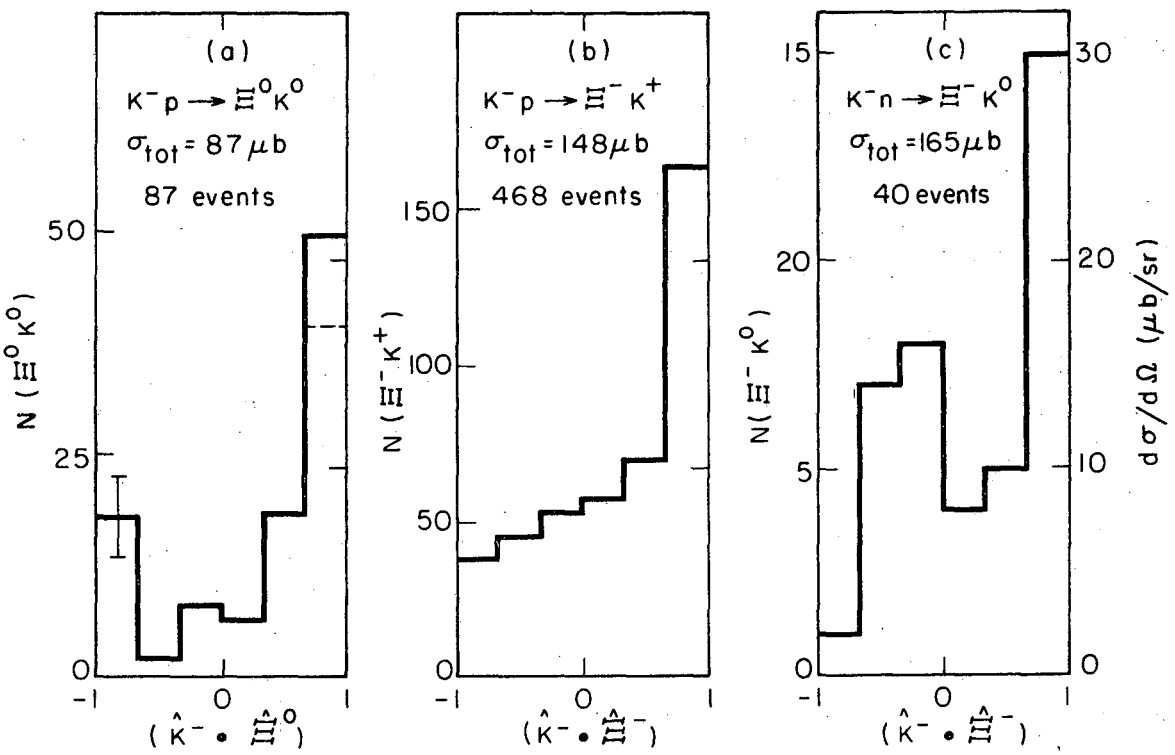

Fig. 7. Differential cross sections at 1.5 BeV/c. (a) $K^- p \rightarrow \Xi^0 K^0$. Data above the broken line in the forward bin were added to the original 87 events by the analysis of 1V2p data for short K^0's. (b) $K^- p \rightarrow \Xi^- K^+$ from Berge et al., Ref. 4. (c) $K^- n \rightarrow \Xi^- K^0$ from Ref. 4. Only deuterium events with spectator-proton momenta below 200 MeV/c are included. Equal areas on the three distributions represent equal cross sections. Scales on the left give numbers of events, on the right, differential cross sections in μb/sr.

0 0 0 0 2 2 0 2 0 6 2

$\Xi^- K^+$ and $\Xi^- K^0$ differential cross sections[4] are also presented in Fig. 7.

C. Exchange Mechanisms

1. Crossing Matrices[22]

For a two-body production reaction, $1 + 2 \rightarrow 3 + 4$, we define the Lorentz invariants:

$$s = (P_1 + P_2)^2 = (P_3 + P_4)^2$$

$$t = (P_1 - P_3)^2 = (P_2 - P_4)^2$$

$$u = (P_1 - P_4)^2 = (P_2 - P_3)^2.$$

Here s is the square of the c.m. energy. The Lorentz-invariant amplitude, A^s, depends only on s, t, and u. We obtain related amplitudes, with t or u as the square of the c.m. energy, by taking other pairs of incoming and outgoing particles. With ΞK production in the s channel, the three production channels are:

$$\begin{aligned} &\text{s channel:} \quad \bar{K}_\alpha + N_\beta \rightarrow K_\gamma + \Xi_\delta \\ &\text{t channel:} \quad \bar{K}_\alpha + \bar{K}_\gamma \rightarrow \bar{N}_\beta + \Xi_\delta \\ &\text{u channel:} \quad \bar{K}_\gamma + N_\beta \rightarrow K_\alpha + \Xi_\delta , \end{aligned} \tag{3.1}$$

where α, β, γ, and δ denote the specific charge states. If strong interactions are CPT-invariant, and if the Lorentz-invariant amplitude is analytic in s, t, and u, the amplitudes for the three reactions are related:

$$\langle K_\gamma \Xi_\delta | A^s | \bar{K}_\alpha N_\beta \rangle = \langle \bar{N}_\beta \Xi_\delta | A^t | \bar{K}_\alpha \bar{K}_\gamma \rangle = \langle K_\alpha \Xi_\delta | A^u | \bar{K}_\gamma N_\beta \rangle. \tag{3.2}$$

In particular, the s and u channels represent the same reaction with the two K's interchanged.

Now consider specific I-spin states. We write an I-spin eigenstate, with magnitude I and z component m, as $|I, m\rangle$. Charge independence in the production process implies

$$\langle I, m | A^s | I', m' \rangle = A_I^s \delta_{II'} \delta_{mm'}, \tag{3.3}$$

with the I-spin amplitude, A_I^s, independent of m. For specific charges, we have

$$\langle K_\gamma \Xi_\delta | A^s | \bar{K}_\alpha N_\beta \rangle = \sum_{I, m} \langle K_\gamma \Xi_\delta | I, m \rangle \langle I, m | A^s | I, m \rangle \langle I, m | \bar{K}_\alpha N_\beta \rangle. \tag{3.4}$$

The projections of the specific charges onto the I-spin eigenstates yield Clebsch-Gordan coefficients,[23] such as $\langle K_\gamma \Xi_\delta | I, m \rangle$. Inverting (3.4), we obtain

$$A_I^s = \langle I, m | A^s | I, m \rangle = \sum_{\alpha\beta\gamma\delta} \langle I, m | K_\gamma \Xi_\delta \rangle \langle K_\gamma \Xi_\delta | A^s | \bar{K}_\alpha N_\beta \rangle \langle \bar{K}_\alpha N_\beta | I, m \rangle, \tag{3.5}$$

which we may evaluate for any m. Now we use (3.2) and the t-channel equivalents of (3.3) and (3.4) to obtain

$$A_I^s = \sum_{I'} A_{I'}^t \{ \sum_{\alpha\beta\gamma\delta} \sum_{m'} \langle I, m | K_\gamma \Xi_\delta \rangle \langle \bar{N}_\beta \Xi_\delta | I', m' \rangle \langle I', m' | \bar{K}_\alpha \bar{K}_\gamma \rangle \langle \bar{K}_\alpha N_\beta | I, m \rangle \}. \tag{3.6}$$

Here $|I', m'\rangle$ is an I-spin eigenstate in the t channel. The quantity in curly brackets is called a "crossing matrix," because it expresses the s-channel amplitudes in terms of the t-channel amplitudes. The crossing matrix contains products of four Clebsch-Gordan coefficients and is proportional to a Racah W-coefficient.[23] For ΞK production, we have

$$A_I^s = \sum_{I'} (-1)^{I+I'+1} (2I'+1)\, W(\tfrac{1}{2}\tfrac{1}{2}\tfrac{1}{2}\tfrac{1}{2}; II')\, A_{I'}^t. \tag{3.7}$$

Interchanging the two K's interchanges the s and u channels.[24] For identical K's, A^u equals A^s. This symmetry under the interchange of identical particles is called "crossing symmetry." More generally, the K-K system is symmetric for I' = 1 and antisymmetric for I' = 0; therefore, interchanging the K's introduces a factor $(-1)^{I'-1}$ in (3.7):

$$A_I^u = \sum_{I'} (-1)^{I+2I'} (2I'+1)\, W(\tfrac{1}{2}\tfrac{1}{2}\tfrac{1}{2}\tfrac{1}{2}; II')\, A_{I'}^t . \qquad (3.8)$$

Equations (3.7) and (3.8) yield

$$A_0^s = (A_0^t + 3A_1^t)/2 = (A_0^u - 3A_1^u)/2$$

and

$$A_1^s = (A_0^t - A_1^t)/2 = -(A_0^u + A_1^u)/2. \qquad (3.9)$$

2. Single-Particle Exchanges

If we allow only single-particle exchanges, we have

$$A_0^s = a_0^s + (a_0^t + 3a_1^t)/2 + (a_0^u - 3a_1^u)/2$$

and

$$A_1^s = a_1^s + (a_0^t - a_1^t)/2 - (a_0^u + a_1^u)/2, \qquad (3.10)$$

where a_I^x is the amplitude for an x-channel exchange with definite I-spin. Due to the crossing symmetry, a_I^s and a_I^u are identical in form. For definite charge states, we obtain

$$A^s(K^-p \to \Xi^0 K^0) = (a_1^s + a_0^s)/2 + (a_1^t + a_0^t)/2 - a_1^u, \qquad (3.11)$$

$$A^s(K^-p \to \Xi^- K^+) = (a_1^s - a_0^s)/2 - a_1^t + (a_1^u - a_0^u)/2, \qquad (3.12)$$

and

$$A^s(K^-n \to \Xi^- K^0) = a_1^s - (a_1^t - a_0^t)/2 - (a_1^u + a_0^u)/2. \qquad (3.13)$$

The crossing symmetry is manifest in (3.12), because the s-channel and u-channel charge states are the same. The s and u channels require an S = -1 baryon; the Λ, Σ, and Y_1^* poles are usually included. The t channel requires an S = 2 meson; there may be evidence for

such a state with I = 1 at 1280 MeV,[25] a mass comparable to the baryon masses. The preponderance of forward Ξ's in Fig. 7 suggests that u-channel baryon exchange is important.

King[26] and Ebel and James[27] have fit $\Xi^- K^+$ data using these pole terms. King concludes that the sharp forward Ξ^- peak requires partial cancellation between the Λ and Σ pole terms. Ebel and James use SU(3) coupling constants[28] at the vertices and obtain complete cancellation of the Λ and Σ poles at f = 0.366, where f is even and d is odd octet coupling, and f + d = 1. When they include mass differences and initial and final-state absorption,[29] they require f > 0.35 to reproduce the forward peak. The SU(6) prediction is f = 0.40 (d/f = 3/2),[30] and analysis of leptonic decay data suggests f = 0.37.[31] King interpreted a small backward Ξ^- peak at 1.7 BeV/c^4 as possible evidence for an I = 1, J = 0, S = 2 meson.[26] Ebel and James chose to ignore the backward peak.[27]

The forward Ξ^0 peak at 1.5 BeV/c is as sharp as the corresponding Ξ^- peaks. The cancellation between Λ and Σ terms invoked for $\Xi^- K^+$ production is inoperative here, because the neutral Λ is absent in the u channel for $K^- p \rightarrow \Xi^0 K^0$. Absorption effects[29] can sharpen both the forward and backward peaks, however. A t-channel exchange of an S = 2 meson could then explain the backward Ξ^0 peak. If the S = 2 meson had I = 1,[25] however, this amplitude would be twice as large in $\Xi^- K^+$ production, where no sharp backward peak appears. Although the two peaks in $\Xi^0 K^0$ production are suggestive, detailed exchange calculations hardly seem warranted. The cross section is still rising from threshold, and dynamic effects are important. Furthermore, the $F_{7/2}$ $Y_1^*(2050)$ and the $G_{7/2}$ $Y_0^*(2100)$ may be important in the direct channel,[32] even though $F_{7/2}$ and $G_{7/2}$ waves are not required in ΞK production at current statistical levels.[4] We have not attempted to incorporate these effects into a full production analysis.

D. SU(n) Symmetry

In the limit of unitary symmetry, when mass differences within the baryon octet and within the meson octet may be neglected,

SU(3) predicts equality for the following amplitudes:[33]

$$A(K^-p \to \Xi^0K^0) = A(K^-p \to \Sigma^-\pi^+) \tag{3.14}$$

$$A(K^-n \to \Xi^-K^0) = A(\pi^-p \to \Sigma^-K^+). \tag{3.15}$$

Meshkov, Snow, and Yodh suggest comparison of relativistically invariant amplitudes at equal Q value, so that the thresholds for additional channels coincide.[34] The square of the amplitude is

$$\bar{\sigma} = (s\, q_{in}/q_{out})\, \sigma, \tag{3.16}$$

where σ is the cross section, q_{in} is the initial and q_{out} the final c.m. momentum, and s is the square of the total c.m. energy.

We study relation (3.14) under the worst possible conditions. The reactions are near threshold, and mass-difference effects are significant. In fact, $K^-p \to \Xi^0K^0$ is endoergic, while $K^-p \to \Sigma^-\pi^+$ is exoergic. Furthermore, the $\Sigma^-\pi^+$ system resonates at the $Y_0^*(1520)$, which is still below threshold for Ξ^0K^0. Comparing total cross sections, we obtain[35]

$$\bar{\sigma}(\Sigma^-\pi^+)/\bar{\sigma}(\Xi^0K^0) \sim 100 \text{ at } Q = 135 \text{ MeV},$$

falling to ~ 10 at Q = 295 MeV.[36] The differential cross sections, on the other hand, are in excellent agreement at Q = 210 MeV (P_{K^-} = 1.5 BeV/c for Ξ^0K^0, 465 MeV/c for $\Sigma^-\pi^+$).

We can superimpose resonances in the $\Sigma\pi$ and ΞK systems by taking equal c.m. energies. The total cross sections still disagree with (3.14). Now $\bar{\sigma}(\Sigma^-\pi^+)/\bar{\sigma}(\Xi^0K^0)$ falls from about 15 at P_{K^-} = 1.2 BeV/c to 2 at P_{K^-} = 1.7 BeV/c.[37]

Relation (3.15) provides a more favorable test, because the kinematics of the two reactions are alike. A deuterium exposure at 1.5 BeV/c yielded 40 Ξ^-K^0(p) events with "spectator" proton momenta below 200 MeV/c; the $K^-n \to \Xi^-K^0$ cross section is (165 ± 34) μb.[4] We compare at equal Q, P_{π^-} = 1.45 BeV/c for Σ^-K^+ production,[14] and obtain

$$\frac{\bar{\sigma}(K^- n \to \Xi^- K^0)}{\bar{\sigma}(\pi^- p \to \Sigma^- K^+)} = \frac{7.0 \times (165 \pm 34)\ \mu b}{6.4 \times (242 \pm 14)\ \mu b} = 0.75 \pm 0.16,$$

with similar angular distributions.

The SU(6) symmetry schemes combine SU(3) multiplets with different spin and obtain, in turn, relations among the ΞK production amplitudes:[38]

$$A(K^- p \to \Xi^0 K^0) = -A(K^- n \to \Xi^- K^0) = -A(K^- p \to \Xi^- K^+)/2. \tag{3.17}$$

These relations are best studied near threshold. High momenta were desirable for (3.14) and (3.15) to mask the differences in masses for the reactions, but here the three reactions involve essentially the same masses. Moreover, SU(6) neglects orbital angular momenta, and the predictions may hold only when S waves are dominant. The $\Xi^0 K^0$ cross section is smaller than the $\Xi^- K^+$ cross section over the range of our experiment.[4] The anisotropic angular distributions at 1.5 BeV/c (Fig. 7), where many of the data lie, are inconsistent with pure S-wave production. The cross sections,

$$\sigma(\Xi^0 K^0) = 87 \pm 11\ \mu b,$$

$$\sigma(\Xi^- K^0) = 165 \pm 34\ \mu b,$$

and

$$\sigma(\Xi^- K^+) = 148 \pm 9\ \mu b,$$

clearly disagree with the prediction, $(\Xi^0 K^0) : (\Xi^- K^0) : (\Xi^- K^+) = 1 : 1 : 4$. We conclude that this energy is too high for the nonrelativistic SU(6) predictions.

The relativistic $SU(6)_W$ description requires (3.17) to hold at all momenta for collinear processes.[39] The $\Xi^- K^+$ intensity at zero and 180 deg must then be four times the corresponding $\Xi^0 K^0$ and $\Xi^- K^0$ intensities. This restriction to collinear events does not improve the agreement with the data in Fig. 7. Jackson suggests that absorption effects break the symmetry by allowing t-channel exchange of the $\underline{35}$ representation, forbidden in pure $SU(6)_W$, but the ΞK relations are not

affected, because the 35 representation does not include an S = 2 meson.[40] Resonances may be important in the s channel, however, as mentioned above. The symmetry requires that the ΞK system resonate simultaneously in all S = -1 members of a given SU(6) baryon multiplet. Therefore, mass splittings within these higher multiplets can upset the symmetry predictions. Furthermore, if the $F_{7/2}$ and $G_{7/2}$ waves associated with the $Y_0^*(2050)$ and the $Y_1^*(2100)$ are important,[32] the amplitudes may vary rapidly near zero and 180 deg, and our data may be too limited to allow an accurate extrapolation to the intensities at the poles. Thus, in this intermediate energy range where s-channel resonances are present, we can test neither the nonrelativistic nor the relativistic symmetry predictions conclusively.

IV. DECAY ASYMMETRY

A. Theory

The amplitude for decay of a spin-J fermion into a spin-1/2 fermion and a spin-zero boson is[41]

$$A = a + b\vec{\sigma} \cdot \hat{q}_f, \tag{4.1}$$

where a is the amplitude for orbital angular momentum $\ell = J - 1/2$, and b for $\ell = J + 1/2$; $\vec{\sigma}$ is the Pauli spin operator, and $\hat{q}_f$ the final fermion's direction in the initial fermion's rest frame. The final-state intensity is

$$I(\hat{q}_i, \hat{q}_f) = I_0(\hat{q}_i)\,(1 + \alpha\vec{P} \cdot \hat{q}_f), \tag{4.2}$$

where the polarization, $\vec{P} = \langle\vec{\sigma}\rangle$, as well as the initial-state intensity, I_0, depends on $\hat{q}_i$, the direction of the initial fermion in its production c.m. The decay-asymmetry parameter is

$$\alpha = 2\mathrm{Re}\, a^* b/(|a|^2 + |b|^2). \tag{4.3}$$

These results apply equally to Ξ and Λ decay.

Consider the decay of a Ξ in its rest frame. Regardless of the spin of the Ξ, its component along the Λ line of flight must equal the Λ helicity, $\pm 1/2$, because no orbital-angular-momentum component is allowed. Figure 8 contains Crawford diagrams and probabilities for the four decay configurations; spins are indicated by double arrows and momenta by displacement.[42] The Ξ spin probabilities, P_+ for ψ_+ and P_- for ψ_-, add to unity, and the Λ helicity probabilities become

$$w_+ = (P_+ + P_-)\,(1 + \alpha_\Xi)/2 = (1 + \alpha_\Xi)/2$$

and

$$w_- = (P_+ + P_-)\,(1 - \alpha_\Xi)/2 = (1 - \alpha_\Xi)/2.$$

The average polarization of the Λ along its line of flight in the Ξ rest frame is then

$$P_\Lambda = (w_+ - w_-)/(w_+ + w_-) = +\alpha_\Xi, \tag{4.4}$$

0 0 0 0 0 0 22 32 0 0 52 66 17 63

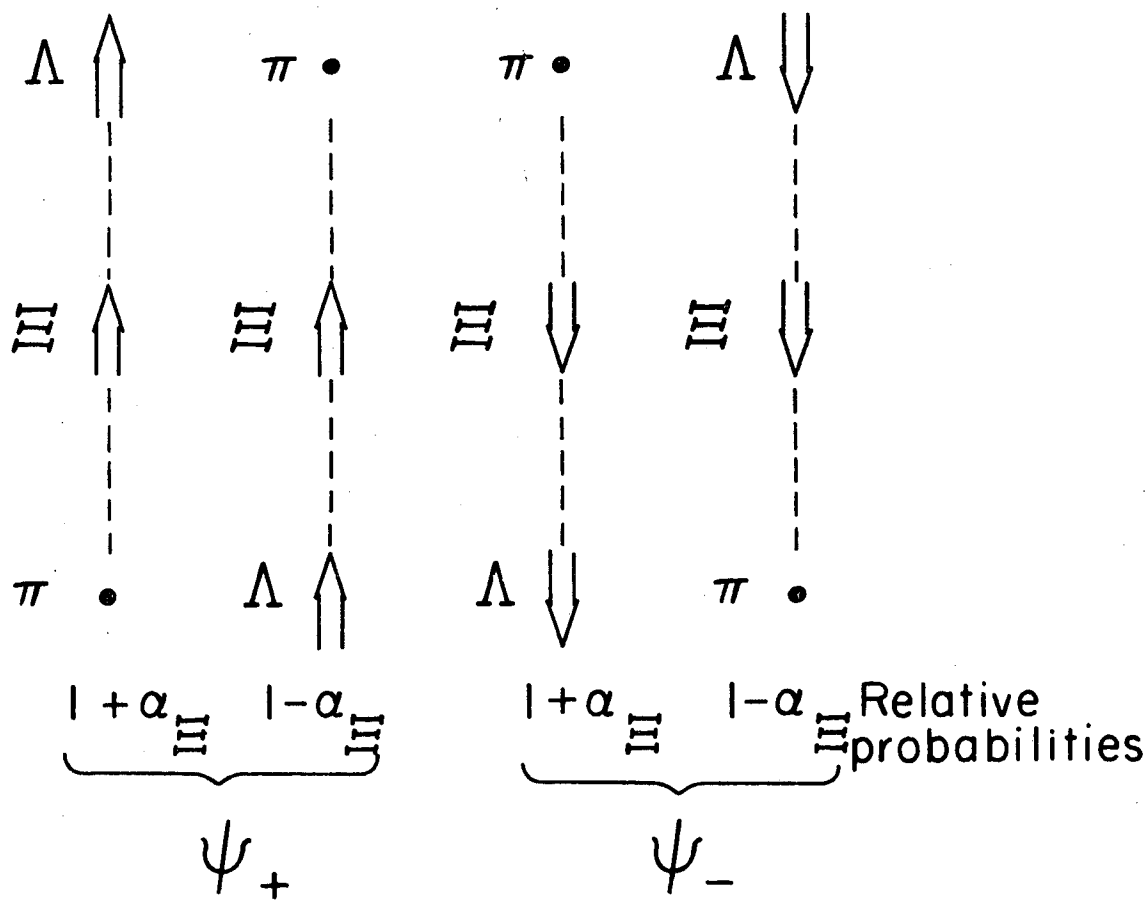

MUB-10504

Fig. 8. Decay configurations in the Ξ rest frame. Double arrows represent intrinsic spins, and positions represent momenta. Relative probabilities of the decays are given for both Ξ initial states, ψ_+ and ψ_-. The Λ must have spin 1/2, but any half-integer Ξ spin is allowed.

independent of the Ξ spin and polarization. Applying (4.2) to the Λ decay, we obtain the well-known spin-independent result,

$$w(\hat{\Lambda} \cdot \hat{p}) = (1 + \alpha_\Lambda \vec{P}_\Lambda \cdot \hat{p})/2 = (1 + \alpha_\Lambda \alpha_\Xi \hat{\Lambda} \cdot \hat{p})/2. \tag{4.5}$$

Here the fermion directions are given in the rest frame of their parent fermions.

B. Results

In Fig. 9 we have plotted $\hat{\Lambda} \cdot \hat{p}$ for the 146 events in our $\Xi^0 K^0$ sample and the 52 events in our $\Xi^0 K^+ \pi^-$ sample. A fit of these $(146+52) = 198$ events to (4.5) yields $\alpha_\Lambda \alpha_{\Xi^0} = -0.13 \pm 0.12$.

Half of the 42 events ambiguous between Ξ^0 production and other production modes give better fits to Ξ^0 production and are included in this sample, as shown in Tables I and IV. Variation of the sample to include or exclude all ambiguous events shifts $\alpha_\Lambda \alpha_{\Xi^0}$ between -0.09 and -0.22. Combining this variation with the statistical uncertainty, we obtain our final result,

$$\alpha_\Lambda \alpha_{\Xi^0} = -0.13 \pm 0.14. \tag{4.16}$$

The corresponding Ξ^- result is[4]

$$\alpha_\Lambda \alpha_{\Xi^-} = -0.245 \pm 0.046. \tag{4.7}$$

The $|\Delta I| = 1/2$ rule[8] for nonleptonic weak decays relates the amplitudes for Ξ^0 and Ξ^- decay:

$$A_{\Xi^0} = -A_{\Xi^-}/\sqrt{2}. \tag{4.8}$$

The amplitudes of each parity satisfy (4.8), and the rule predicts $\alpha_{\Xi^0} = \alpha_{\Xi^-}$. Our result, $\alpha_{\Xi^0}/\alpha_{\Xi^-} = 0.5 \pm 0.6$, agrees with this prediction, even though α_{Ξ^0} is also consistent with zero. With $\alpha_\Lambda = 0.66 \pm 0.05$,[19] we obtain $\alpha_{\Xi^0} = -0.20 \pm 0.22$; the latest world compilation for the Ξ^- gives $\alpha_{\Xi^-} = -0.41 \pm 0.05$.[19]

0 0 0 0 2 2 3 2 0 0 3 2 6 6 1 7 7 4

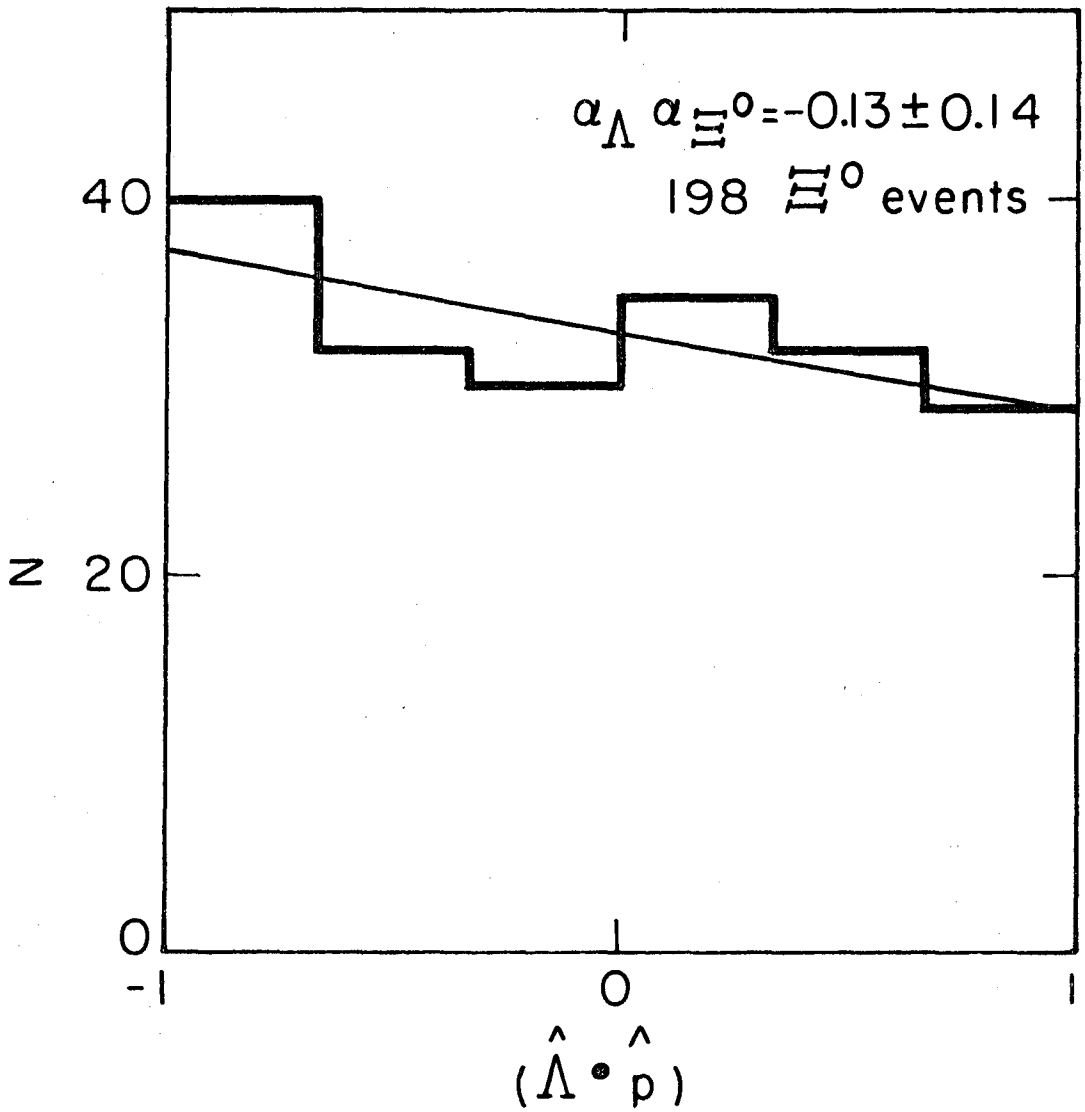

MUB-10503

Fig. 9. Decay asymmetry. The straight line is a fit to $(1 + \alpha_\Lambda \alpha_{\Xi^0} \hat{\Lambda} \cdot \hat{p})$. The distribution contains 198 events: 146 $\Xi^0 K^0$ and 52 $\Xi^0 K^+ \pi^-$.

V. LIFETIME

A. Restrictions on Sample

The lifetime analysis was restricted to events that exhibit the full two-body $\Xi^0 K^0$ production and decay chain of (2.1). The $\Xi^0 K^0 \pi^0$ events are poorly determined and yield an imprecise Ξ^0 length determination. The $\Xi^0 K^+ \pi^-$ events were selected from 1V2p events that failed more common production modes, such as $K^- p \rightarrow \Lambda \pi^+ \pi^- \pi^0$. As discussed in section II, this 1V2p analysis suffers a bias against short Ξ^0 proper times, because the Λ must point to the primary vertex for non-Ξ^0 production.

The data with beam momenta below 1.3 BeV/c were also excluded from this analysis. According to Table II, the majority of 2V0p events at these lower momenta were produced by π^- contamination. The addition of these events would increase the uncertainty in our final result.

The 2V0p topological sample at 1.3 BeV/c and above contains 190 events: 137 $\Xi^0 K^0$ events, 8 $\Xi^0 K^0 \pi^0$ events, and 45 productions by π^- contamination. Seventeen of these events are ambiguous between $\Xi^0 K^0$ production and some other mode; eleven of the ambiguous events are included in the present sample of 137 $\Xi^0 K^0$ events.

B. Calculation of Ξ^0 Length

The Ξ^0 length is determined from the fitted data by geometric construction,

$$\ell_{\Xi^0} = \ell_X \sin\alpha_2 / \sin\theta, \qquad (5.1)$$

as discussed in section II. The link (X) and the angles are shown schematically in Fig. 4. The calculated length need not be positive; its average uncertainty is about 1 cm.

Five events in the sample allow direct measurement of the Ξ^0 decay point, because the π^0 (from $\Xi^0 \rightarrow \Lambda \pi^0$) decays in the Dalitz mode, $\pi^0 \rightarrow \gamma e^+ e^-$. These decay points were also calculated from (5.1), after discarding all information from the Dalitz pair. The calculated lengths averaged 15% higher than the measured lengths, consistent with the expected error (1.5 standard deviations).

In the following analysis, the uncertain Ξ^0 length is varied while the well-measured link is kept fixed. The concomitant variation of the Λ length must be considered. The link is related to the fermion lengths by

$$\ell_X = \ell_{\Xi^0} \cos\alpha_1 + \ell_\Lambda \cos\alpha_2, \tag{5.2}$$

where $\cos\alpha_1 = \hat{\Xi}^0 \cdot \hat{X}$ and $\cos\alpha_2 = \hat{\Lambda} \cdot \hat{X}$. These coefficients must vary with ℓ_{Ξ^0}, because the link plus the two angles determine the triangle. Furthermore, we imagine a trajectory for the Ξ^0 and Λ such that the link direction is unchanged. Now either the Ξ^0 production angle or the Ξ^0 decay angle must also change, and kinematic constraints require changes in momenta. This situation can be simplified with little loss of accuracy, however, because θ, the Ξ^0 decay angle in the laboratory system, is small, ≤ 20 deg, as discussed in connection with Eq. (2.5). The length of the link is then very nearly (within 2%) the sum of the fermion lengths, and the exact variation of ℓ_Λ, as ℓ_{Ξ^0} varies from zero to ℓ_X, is not critical.

C. Likelihood Formulation

The calculated Ξ^0 length and the fitted momentum provide a convenient determination of the Ξ^0 proper time,

$$t_{\Xi^0} = \ell_{\Xi^0}/\eta_{\Xi^0}, \tag{5.3}$$

with $\eta_\Xi = p_\Xi/M_\Xi$ and $c = 1$. We determine the Ξ^0 mean life from the distribution of proper times in Fig. 10. Even if the Ξ^0 length were not known, however, we could determine the Ξ^0 mean life from the lengths of the links.

If the Ξ^0 length is accurately measured, the joint probability, for the kth event, of observing proper times $t_{1k} = \ell_{1k}/\eta_{1k}$ for a Ξ^0 with decay rate $\lambda_1 = \tau_{\Xi^0}^{-1}$ and $t_{2k} = \ell_{2k}/\eta_{2k}$ for a Λ with $\lambda_2 = \tau_\Lambda^{-1}$ is

$$P_k(t_{1k}, t_{2k}; \lambda_1, \lambda_2) = f_k(\lambda_1, \lambda_2)\lambda_1\lambda_2 \exp(-\lambda_1 t_{1k} - \lambda_2 t_{2k}). \tag{5.4}$$

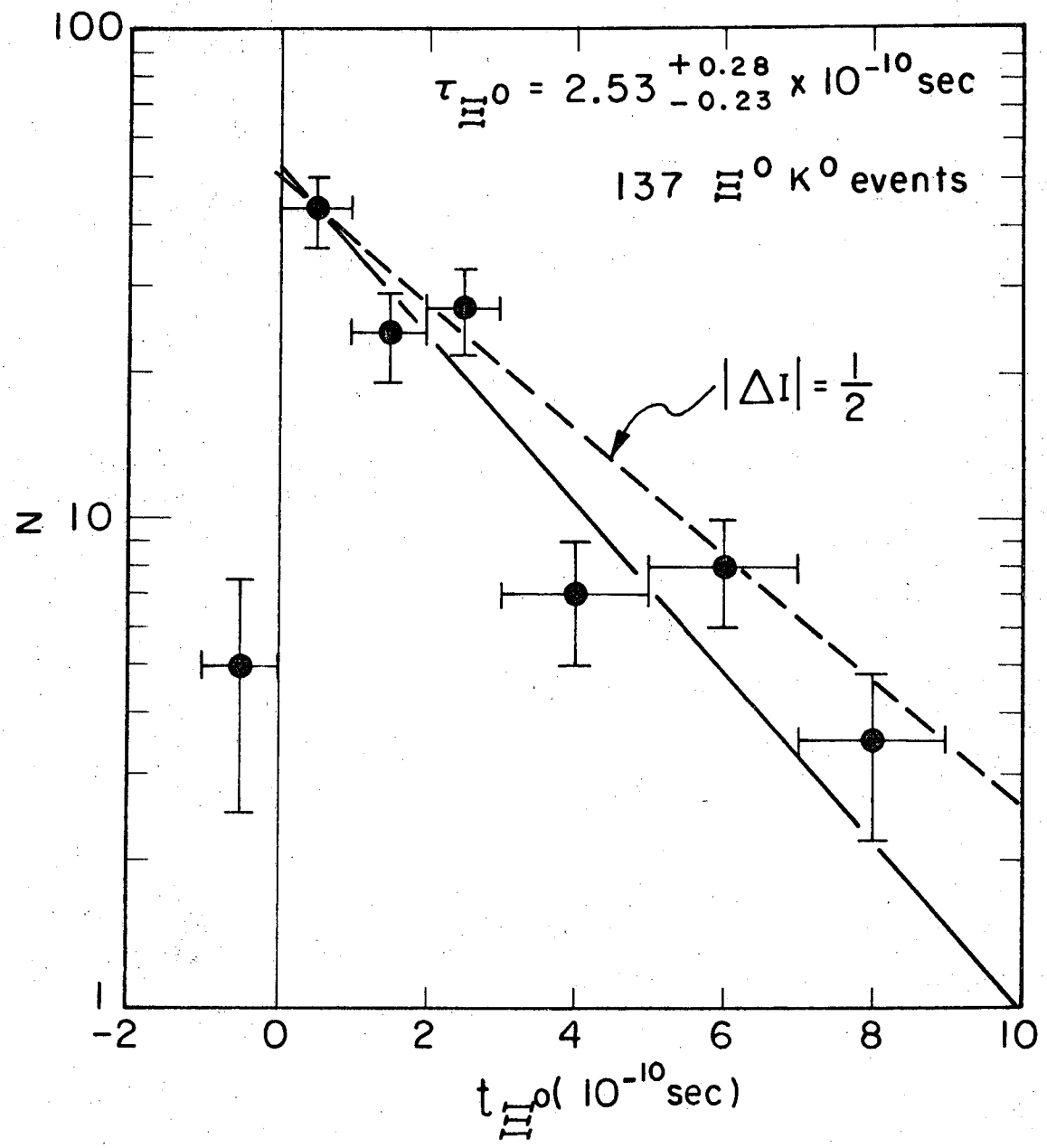

MUB-10501

Fig. 10. Ξ^0 lifetime distribution. The data points are not corrected for detection efficiency or the uncertainty in the length calculations. The slope of the solid line is $\lambda_{\Xi^0} = 1/(2.53 \times 10^{-10}$ sec). The slope of the broken line is $\lambda_{\Xi^0}/2$, the $|\Delta I| = 1/2$ prediction. Note that five calculated proper times are negative.

For an infinite bubble chamber, the decay rates are separable, but for a finite chamber, they are coupled through the normalization term,

$$f_k^{-1}(\lambda_1, \lambda_2) = \lambda_1\lambda_2 \int_0^{\beta_{1k}} dt_1 \int_{\alpha_{2k}(t_1)}^{\beta_{2k}(t_1)} dt_2 \exp(-\lambda_1 t_1 - \lambda_2 t_2). \quad (5.5)$$

The maximum Ξ^0 proper time is $\beta_{1k} = b_{1k}/\eta_{1k}$, where b_{1k} is the distance along the Ξ^0 line of flight to the nearest boundary. The allowable t_2 depend on t_1. In particular, the minimum Λ length decreases as t_1 increases, so that the minimum link is 0.5 cm.

In fact, the measured Ξ^0 length, ℓ_{1k}, has an appreciable uncertainty,[43] σ_{1k}. On the other hand, the length of the link, ℓ_{3k}, is accurately measured, with an uncertainty small relative to 0.5 cm, its minimum length. We take the Ξ^0 length measurements to be normally distributed about the true values and fold a Gaussian error function into the probability function. Equation (A.6) of the appendix presents the probability, $P_k^{Q'}(\ell_{1k}, \ell_{3k}; \lambda_1, \lambda_2)$, for this pair of measurements. The combined likelihood for N events is

$$\mathcal{L}^Q(\lambda_1, \lambda_2) = \prod_{k=1}^{N} P_k^{Q'}(\ell_{1k}, \ell_{3k}; \lambda_1, \lambda_2). \quad (5.6)$$

If the Ξ^0 and Λ are collinear, the Ξ^0 length is undetermined. The link then provides the only information in the joint probability function, $P_k^{Q'}(\ell_{1k}, \ell_{3k}; \lambda_1, \lambda_2)$, and a new formulation is appropriate. At our momenta this formulation can determine the Ξ^0 lifetime, because all events are nearly collinear in the laboratory. We express the probability in terms of the sum of the fermion lengths, $\ell_{1k} + \ell_{2k} \approx \ell_{3k}$, and their difference, then integrate over the difference. The result, $P_k^X(\ell_{3k}; \lambda_1, \lambda_2)$, is given in (A.10). The corresponding likelihood function is $\mathcal{L}^X(\lambda_1, \lambda_2)$.

D. Results

The likelihood function, $\mathcal{L}^Q(\lambda_1, \lambda_2)$ in (5.6) was maximized as a function of the Ξ^0 lifetime only. We obtain $\tau_{\Xi^0} = 2.53^{+0.26}_{-0.21} \times 10^{-10}$ sec.

This result is insensitive to the Λ lifetime assumed. We used $\tau_\Lambda = 2.59 \times 10^{-10}$ sec;[6] variation of τ_Λ from 2.45×10^{-10} sec to 2.7×10^{-10} sec shifts τ_{Ξ^0} by less than 0.01×10^{-10} sec.

The alternate function, $\mathcal{L}^X(\lambda_1, \lambda_2)$, ignores the calculated Ξ^0 length. As we vary τ_Λ, τ_{Ξ^0} varies so that the sum of the Ξ^0 and Λ decay rates remains roughly constant. Using $\tau_\Lambda = 2.59 \times 10^{-10}$ sec, we obtain $\tau_{\Xi^0} = 2.71^{+0.40}_{-0.31} \times 10^{-10}$ sec. This result constitutes a successful check on the consistency of our data.

As mentioned above, we include eleven of the seventeen ambiguous events in our sample. Including all seventeen ambiguous events in (5.6), we have $\tau_{\Xi^0} = 2.41 \times 10^{-10}$ sec; excluding all seventeen, $\tau_{\Xi^0} = 2.67 \times 10^{-10}$ sec. Combining this variation with the statistical and measurement uncertainties, we obtain our final result, for 137 $\Xi^0 K^0$ events:

$$\tau_{\Xi^0} = 2.53^{+0.28}_{-0.23} \times 10^{-10} \text{ sec.}$$

Two independent determinations of τ_{Ξ^0} have been presented: Jauneau et al. obtain $3.8^{+1.0}_{-0.7} \times 10^{-10}$ sec with 25 events;[44] Carmony et al. obtain $3.5^{+1.0}_{-0.8} \times 10^{-10}$ sec with 54 events.[45] There is no statistically significant disagreement among our results.

The ratio of the Ξ^0 and Ξ^- decay rates provides another test of the $|\Delta I| = 1/2$ rule.[8] We compare our result with the Ξ^- result from the same experiment,[6] $\tau_{\Xi^-} = 1.69 \pm 0.06 \times 10^{-10}$ sec, and obtain $\lambda_{\Xi^0}/\lambda_{\Xi^-} = 0.67 \pm 0.08$, two standard deviations from the prediction of 0.5. The $|\Delta I| = 1/2$ prediction, as well as our best-fit result, is displayed with the proper time distribution in Fig. 10.

0 0 0 0 22 32 0 32 5 27 07

VI. RARE DECAY MODES

A. Dalitz Events

The branching ratio for the Dalitz decay mode[46] of the π^0, $\pi^0 \to \gamma e^+ e^-$, is $(1.17 \pm 0.05)\%$.[47] This rate is independent of the π^0 production mode. Figure 11 shows a Ξ^0 Dalitz event:

$$K^- + p \to \underbrace{\Xi^0 \to \underbrace{\Lambda \to \underbrace{p + \pi^-}} + \underbrace{\pi^0 \to \underbrace{\gamma + e^+ + e^-}}}_{} + \underbrace{K^0 \to \underbrace{\pi^+ + \pi^-}}_{} \tag{6.1}$$

The π^0 lifetime is about 10^{-16} sec; therefore, the Dalitz pair (e^+e^-) marks the Ξ^0 decay point.

Among our 206 Ξ^0 events we expect 2.5 Dalitz events and observe eight: five $\Xi^0 K^0$, one $\Xi^0 K^0 \pi^0$, and two $\Xi^0 K^+ \pi^-$.[48] The probability for observing eight or more Dalitz events in our sample is 0.4%. This abundance of electron pairs may be due to a statistical fluctuation or a new Ξ^0 decay mode.

The $\Xi^0 K^0$ events with unseen K^0 decays are not included in the sample above. They provide a check for fluctuations. The $(2 \times 146) = 292$ such $\Xi^0 K^0$ events with visible Λ's yield three Dalitz events, where 3.5 are expected. We conclude that the excess of Dalitz events could be a statistical fluctuation.

On the other hand, these events could arise from a second π^0. A pion with spin, the spion, was suggested by Cvijanovich et al.[49] to save time-reversal invariance from violation in the decay $K_L^0 \to \pi^+\pi^-$.[50] The spin of this spion was to explain observed asymmetries in the $\pi^\pm$ and K^+ decays, but the branching ratios disagree with the predictions for charged spions.[51] Neutral spions should decay predominantly into $\gamma e^+ e^-$ if $J = 1$, because decay into two γ's would be forbidden.[52]

The kinematic properties of the π^0 Dalitz decay are well known.[47,53] The electron pair comes from a virtual transverse photon, and its invariant mass is small. In contrast, an electron pair in spion decay cannot come from a single virtual photon,[54] and the electron-pair mass may be large. The invariant masses for our eight

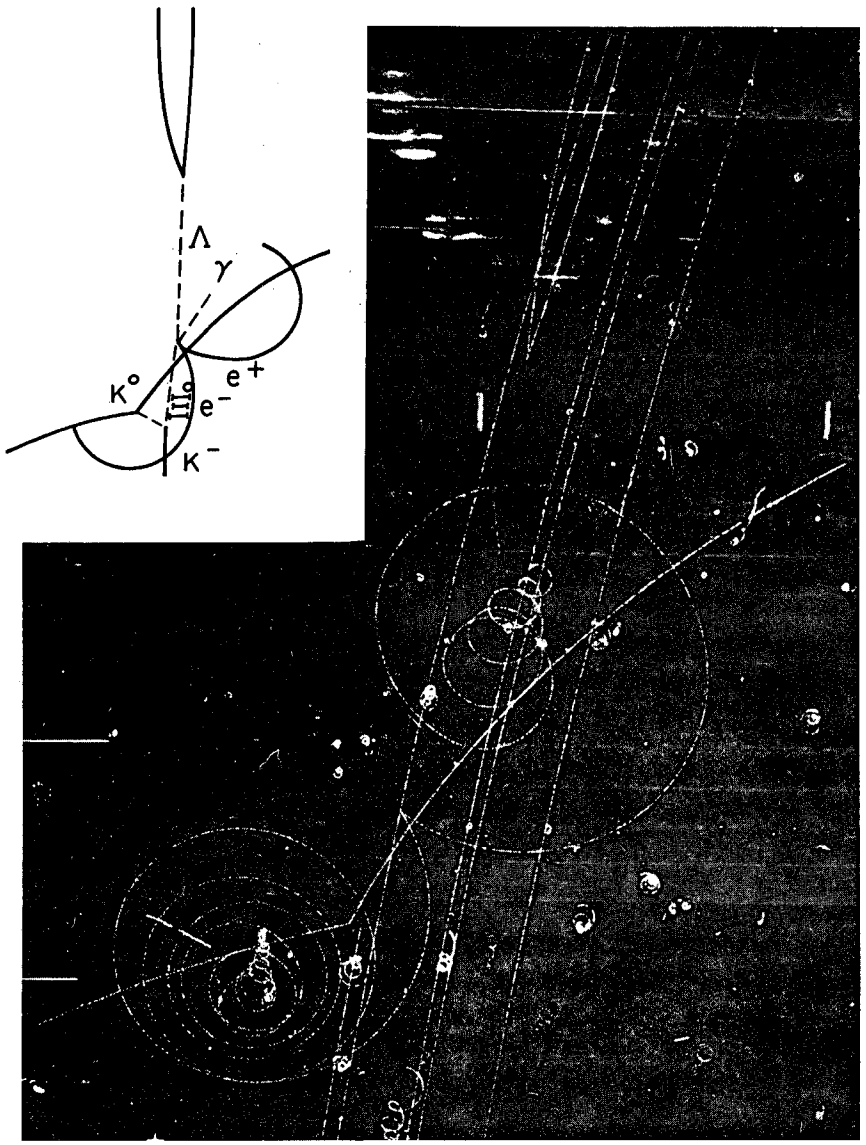

ZN-5480

Fig. 11. Example of a Dalitz event: $K^- + p \rightarrow \Xi^0 + K^0$, $\Xi^0 \rightarrow \Lambda + \pi^0$, $\pi^0 \rightarrow \gamma + e^+ + e^-$. The electron pair marks the Ξ^0 decay point, because the π^0 lifetime is very short.

00 00 00 00 22 32 00 52 65 27 18

events are shown in Fig. 12, together with the phase space expected for π^0 Dalitz events. These results are clearly consistent with pure π^0 decay of the Ξ^0.

B. Other Ξ^0 Decay Modes

We searched for other Ξ^0 decay modes: the $\Delta S = 1$ leptonic decays with $\Delta S/\Delta Q = +1$,

$$\Xi^0 \to \Sigma^+ + e^- + \bar{\nu} \qquad \text{(A)}$$

$$\Xi^0 \to \Sigma^+ + \mu^- + \bar{\nu}, \qquad \text{(B)}$$

and with $\Delta S/\Delta Q = -1$,

$$\Xi^0 \to \Sigma^- + e^+ + \nu \qquad \text{(C)}$$

$$\Xi^0 \to \Sigma^- + \mu^+ + \nu; \qquad \text{(D)}$$

the direct, nonleptonic, $\Delta S = 2$ decay,

$$\Xi^0 \to p + \pi^-; \qquad \text{(E)}$$

and the $\Delta S = 2$ leptonic decays,

$$\Xi^0 \to p + e^- + \bar{\nu} \qquad \text{(F)}$$

$$\Xi^0 \to p + \mu^- + \bar{\nu}. \qquad \text{(G)}$$

No definite examples of these decay modes were found. Upper limits are based on our 146 $\Xi^0 K^0$ events, corrected for neutral Λ decays.

1. Theory

The weak interaction Lagrangian is often described as the self-coupling of a single charged current, J_μ, with vector and axial-vector terms in space-time:[55]

$$\mathcal{L}_w = (1/\sqrt{2})\, G_w J^\dagger_\mu J_\mu, \qquad (6.2)$$

where G_w is the weak coupling constant, and

$$J_\mu = j_\mu + S_\mu + \ell_\mu. \qquad (6.3)$$

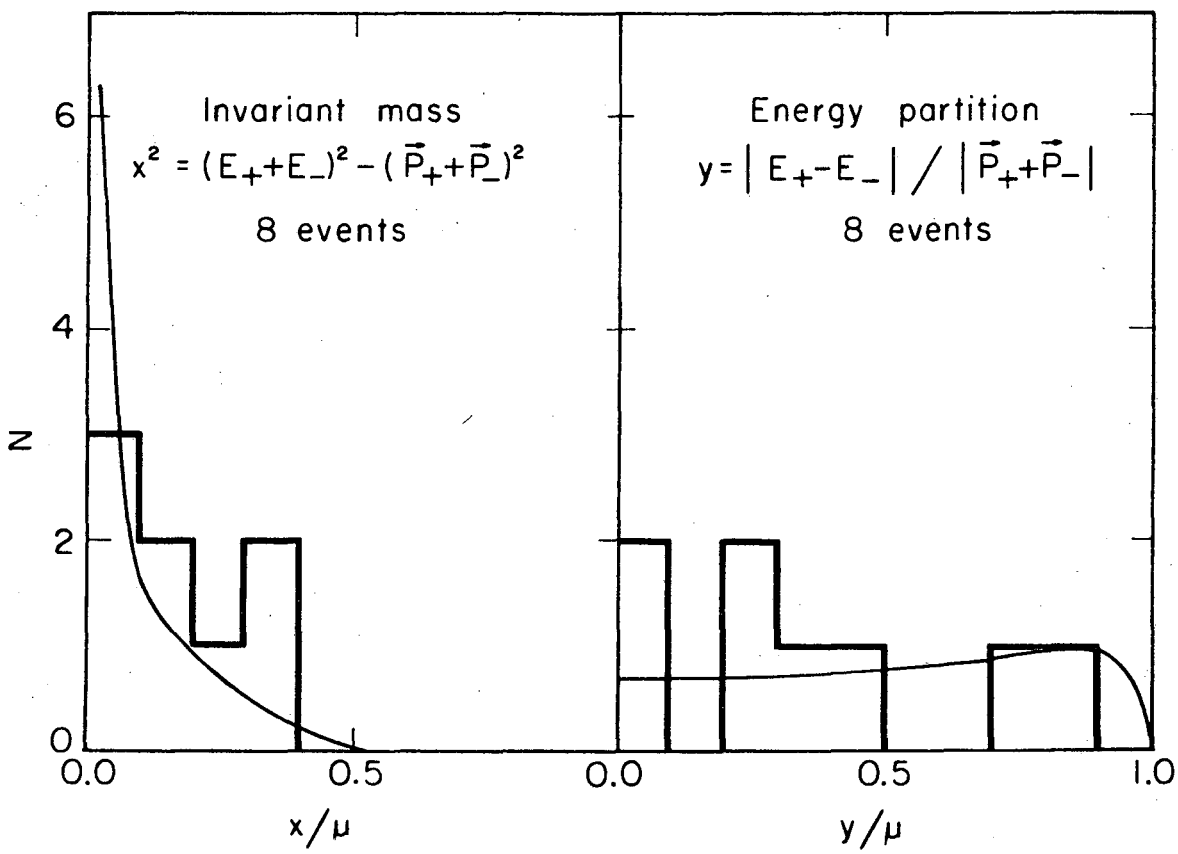

MUB-10505

Fig. 12. Invariant mass and energy partition for electron pairs in Dalitz events in units of μ, the π^0 mass. The smooth curves are expected for π^0 decay, $\pi^0 \rightarrow \gamma + e^+ + e^-$.

Here j_μ is the strangeness-conserving, and S_μ the strangeness-changing, current of strongly interacting particles, and ℓ_μ is the current of leptons. (We write $\ell^\pm$ for the leptons to signify both $e^\pm$ and $\mu^\pm$.) To produce well-established decays such as $\Lambda \to pe^-\bar{\nu}$, S_μ must have a term with $\Delta S = \Delta Q$. If S_μ contains no other terms, Ξ^0 decay modes (A) and (B) are allowed, but not (C) through (G), to first order in G_w.

In this sense, the $\Delta S = 1$, $\Delta S/\Delta Q = +1$ leptonic decays, $\Xi^0 \to \Sigma^+\ell^-\bar{\nu}$, are the only fully respectable modes on our list. They are included in the fashionable Cabibbo theory,[56] in which j_μ and S_μ transform like members of an SU(3) octet. The (D/F) ratios for the vector and axial-vector currents determine the form for each decay. The vector current has pure antisymmetric F coupling, and it is conserved.[55] Two new parameters are $\tan\theta$, the relative strength of S_μ and j_μ, and $(D/F)_A$, the ratio of the axial-vector octet couplings. The Ξ^0 decay (A) has the V-A form of neutron β decay regardless of $(D/F)_A$, and the ratio of the Ξ^0 amplitude to the neutron amplitude is $\tan\theta$.

Inclusion of SU(6) with the Cabibbo theory requires[30] $(D/F)_A = 3/2$, which is consistent with experiment,[31] and $G_A/G_V = 5/3$, which is not. Gell-Mann's equal-time commutation relations[57] for the vector and axial-vector currents in SU(3) reproduce these SU(6) results, with bare couplings.[58] When renormalization is included,[59] both $(D/F)_A$ and G_A/G_V agree with the experimental values.[31]

The $\Delta S/\Delta Q = -1$ decays, $\Xi^0 \to \Sigma^-\ell^+\nu$, would require a new term in S_μ. The coupling of this $\Delta S = -\Delta Q$ term to the $\Delta S = +\Delta Q$ term would produce nonleptonic $\Delta S = 2$ transitions, such as $\Xi^0 \to p\pi^-$ and $K^0 \rightleftarrows \bar{K}^0$. But the $K_1^0 - K_2^0$ mass difference[60] is inconsistent with first-order $K^0 \rightleftarrows \bar{K}^0$ transitions.[61] One proposal to explain the CP-violating $K_L^0 \to \pi^+\pi^-$ decay[50] is a superweak $\Delta S = -\Delta Q$ term, with an amplitude $\sim 10^{-9}$ times the $\Delta S = \Delta Q$ term.[62] The attendant leptonic $\Delta S = -\Delta Q$ decays and nonleptonic $|\Delta S| = 2$ decays would be suppressed by a factor $\sim 10^{-18}$.

We can accommodate $\Delta S/\Delta Q = -1$ decays without $\Delta S = 2$ transitions by including two charged currents,[63]

$$\mathcal{L}_w = (1/\sqrt{2})\, G_w \sum_i J_\mu^{(i)\dagger} J_\mu^{(i)}, \tag{6.4}$$

so that the $\Delta Q = -\Delta S$ term does not couple to the $\Delta Q = +\Delta S$ term. Alternatively, the intermediate-vector-boson model requires at least two distinct charged bosons.[64] One probable $\Delta S = -\Delta Q$ decay, $\Sigma^+ \to n\mu^+\nu$, has been observed,[65] but the $\Delta S = -\Delta Q$ rate is less than 10% of the $\Delta S = \Delta Q$ rate.[66]

Next, $\Delta S = 2$ terms have been added to one of the charged currents so that only leptonic $\Delta S = 2$ interactions are allowed.[67] Phase space for $\Xi^0 \to p\ell^-\bar{\nu}$ is large, and branching ratios of a few percent might be expected.

Finally, Glashow has shown that nonleptonic $\Delta S = 2$ interactions can produce $\Xi^0 \to p\pi^-$ decays without first-order contributions to the $K_1^0 - K_2^0$ mass difference.[68] In the single self-coupling current model, this interaction must violate CP invariance.[69] The $K_L^0 \to \pi^+\pi^-$ decay rate[50] then suggests a rate for the $\Delta S = 2$ decays $\sim 10^{-4}$ to 10^{-6} times the rate for $\Delta S = 1$ decays.[70]

The decay rate for leptonic decays with pure vector (G_V) and axial-vector (G_A) coupling is[71]

$$\lambda = (1/60\pi^3)\,(1 + M_1/M_2)^3\, Q^5\, B(\eta)\, [G_V^2 + 3G_A^2], \tag{6.2}$$

where M_1 is the initial and M_2 the final baryon mass, $Q = M_1 - M_2$, and $\eta = (\mu/Q)^2$, with μ the lepton mass. The phase-space dependence on the lepton mass,

$$B(\eta) = (1-\eta)^{1/2}\,(1 - 9\eta/2 - 4\eta^2) + (15/4)\eta^2 \ln\left|[1 + (1-\eta)^{1/2}]/[1 - (1-\eta)^{1/2}]\right|, \tag{6.3}$$

inhibits decay into heavy leptons. With e, μ universality the rates for corresponding electronic and muonic decays differ only by this phase-space factor, which inhibits the $\Delta S = 1$ muonic decays (B and D) by a factor of 0.002, and the $\Delta S = 2$ muonic decay (G) by a factor of 0.60.

2. Results

We searched for Ξ^0 decay modes (A) through (G) among the events with the 2V0p topology. These decays require that the Ξ^0

direction coincide with the measured link. Sixty-five of the 221 2V0p events fit $\Xi^0 K^0$ production with this restriction and are candidates for these decay modes.

The $\Delta S = 1$ leptonic decays, $\Xi^0 \to \Sigma^{\pm} \ell^{\mp} \nu$, and the $\Delta S = 2$ nonleptonic decay, $\Xi^0 \to p\pi^-$, are unambiguous; no serious candidates for these modes were discovered. The $\Delta S = 2$ leptonic decay modes can be ambiguous with the usual cascade, $\Xi^0 \to \Lambda\pi^0$, $\Lambda \to p\pi^-$. Sixteen of the 65 candidate events fit $\Xi^0 \to p\mu^-\bar{\nu}$; ten of these also fit $\Xi^0 \to pe^-\bar{\nu}$; all sixteen fit the usual cascade decay. We eliminate events if the calculated mass of the vee is within three standard deviations of the Λ mass, assuming proton and π^- tracks. From the leptonic decay spectrum,[71] we estimate that 7% of the electronic events and 10% of the muonic events would be discarded. No candidates remain.

Minimum lengths for the Ξ^0 and $\Sigma^{\pm}$ were 0.5 cm; the failure rates are 8% for Ξ^0, 22% for Σ^+, and 12% for Σ^-. The 221 2V0p events include 146 $\Xi^0 K^0$ events. The upper limits are:

$$R_A(\Xi^0 \to \Sigma^+ e^- \bar{\nu}) < 1/(0.92 \times 0.78 \times 1.5 \times 146) \simeq 0.7\%$$

$$R_B(\Xi^0 \to \Sigma^+ \mu^- \bar{\nu}) < 1/(0.92 \times 0.78 \times 1.5 \times 146) \simeq 0.7\%$$

$$R_C(\Xi^0 \to \Sigma^- e^+ \nu) < 1/(0.92 \times 0.88 \times 1.5 \times 146) \simeq 0.6\%$$

$$R_D(\Xi^0 \to \Sigma^- \mu^+ \nu) < 1/(0.92 \times 0.88 \times 1.5 \times 146) \simeq 0.6\%$$

$$R_E(\Xi^0 \to p\pi^-) < 1/(0.92 \times 1.5 \times 146) \simeq 0.5\%$$

$$R_F(\Xi^0 \to pe^- \bar{\nu}) < 1/(0.93 \times 0.92 \times 1.5 \times 146) \simeq 0.6\%$$

$$R_G(\Xi^0 \to p\mu^- \bar{\nu}) < 1/(0.90 \times 0.92 \times 1.5 \times 146) \simeq 0.6\%.$$

The Cabibbo theory predicts[56] 0.28% for $\Xi^0 \to \Sigma^+ e^- \bar{\nu}$. Other predictions are generally less precise, but are of the same order of magnitude. More statistics are needed to test these theories. We do have some evidence against the $\Delta S = 2$ leptonic theories,[67] however.

We have reported elsewhere the search for Ξ^- leptonic decays.[4] The sole candidate for $\Xi^- \to \Lambda \ell^- \bar{\nu}$ is more probably a normal decay, $\Xi^- \to \Lambda \pi^-$. Our upper limits for $\Delta S = 1$, $\Delta S/\Delta Q = +1$ leptonic Ξ^- decays are:

$$R(\Xi^- \to \Lambda e^- \bar{\nu}) \leq 0.5\%$$

$$R(\Xi^- \to \Lambda \mu^- \bar{\nu}) \leq 1.2\%$$

$$R(\Xi^- \to \Sigma^0 e^- \bar{\nu}) < 0.3\%$$

$$R(\Xi^- \to \Sigma^0 \mu^- \bar{\nu}) < 0.5\%.$$

Ferro-Luzzi et al. set an upper limit on the $\Delta S = 2$ nonleptonic Ξ^- decay from this experiment,[7]

$$R(\Xi^- \to n\pi^-) < 0.5\%.$$

The only unusual Ξ decays reported to date are Ξ^- leptonic decays, $\Xi^- \to \Lambda e^- \bar{\nu}$. Carmony and Pjerrou report one such event with a branching ratio of about 0.6%.[72] London et al. observe one definite and one probable leptonic Ξ^- among 164 decays.[73] Our upper limit[4] at 0.5% is consistent with these results.

0 0 0 0 0 0 2 2 3 2 0 0 5 2 5 2 8 4 1

ACKNOWLEDGMENTS

I appreciate the guidance of Prof. M. Lynn Stevenson; he has shown personal concern during the critical periods of my graduate career. I also appreciate the close associations with Dr. J. Peter Berge and Peter G. Wohlmut; they have contributed generously their time and effort throughout this analysis.

Prof. Harold K. Ticho (UCLA) supervised the beam design and construction. Drs. Frank T. Solmitz and Margaret Alston did much of the early analysis of the Ξ^0 events. Many members of the Alvarez Group helped me through frequent discussions. Dr. Charles G. Wohl has been an especially close associate.

Much of the toil has fallen upon the staff of the Lawrence Radiation Laboratory. Dennis Byrnes and David Enfield performed scanning projects, supervised by Peter G. Wohlmut and Jacob Neufeld. Roger Griswold and Robert Good expedited computer operations. Joyce Spikes performed secretarial duties, and Janice M. Hirota, special services. I am grateful to these and to many other members of the staff who have contributed their labor to this work.

Finally, I acknowledge with pleasure the support and encouragement of Prof. Luis W. Alvarez.

This work was done under the auspices of the U. S. Atomic Energy Commission.

APPENDIX. LIFETIME LIKELIHOOD FORMULATION

A schematic diagram of Ξ^0 production and decay, illustrating the link from the production vertex to the Λ decay, is presented in Fig. 4. As discussed in section V, the Ξ^0 decay rate may be determined either from the calculated Ξ^0 lengths or from the measured links, ignoring the Ξ^0 lengths. The likelihood functions for these two cases are developed as follows.

1. Lifetime from the Ξ^0 Length

The joint probability, for the kth event, of observing proper times t_{1k} for a Ξ^0 with decay rate $\lambda_1 = \tau_{\Xi^0}^{-1}$ and t_{2k} for a Λ with $\lambda_2 = \tau_\Lambda^{-1}$ is given by (5.4). The lengths are proportional to the proper times; with $\eta = p/M$ and $c = 1$, we have $\ell = \eta t$.

Next, we allow for uncertainty in the Ξ^0 length. Let the limits on the true lengths be $A \leqslant x \leqslant B$ and the limits on the measured lengths be $a \leqslant \ell \leqslant b$, suitably subscripted. The maximum lengths, true and measured, are set by the distances to the nearest boundaries. The minimum true lengths are zero. The minimum measured Ξ^0 length, a_{1k}, is negative, as previously mentioned, and equal to the distance from the primary vertex backwards to the nearest boundary. The cutoff at 0.5 cm for the link restricts the range of measurements, not of true lengths.

The probability that the true lengths be x_1 for the Ξ^0 and x_2 for the Λ is

$$P_k(x_1, x_2; \lambda_1, \lambda_2) = f_k(\lambda_1, \lambda_2)\,(\lambda_1\lambda_2/\eta_{1k}\eta_{2k})\exp(-\lambda_1 x_1/\eta_{1k} - \lambda_2 x_2/\eta_{2k}), \tag{A.1}$$

with

$$f_k^{-1}(\lambda_1, \lambda_2) = (\lambda_1\lambda_2/\eta_{1k}\eta_{2k}) \int_0^{B_{1k}} dx_1 \int_0^{B_{2k}(x_1)} dx_2 \exp(-\lambda_1 x_1/\eta_{1k} - \lambda_2 x_2/\eta_{2k}). \tag{A.2}$$

This probability is normalized over the range of true Ξ^0 and Λ lengths. The Jacobian factor $(\eta_{1k}\eta_{2k})$ has been included explicitly in (A.1), so that $f_k(\lambda_1, \lambda_2)$ is one for an infinite bubble chamber.

The true length of the link is $x_3 = x_1\mu_1 + x_2\mu_2$, where $\mu_1 = \hat{\Xi}^0 \cdot \hat{X}$ and $\mu_2 = \hat{\Lambda} \cdot \hat{X}$. As discussed in connection with (5.2), μ_1 and μ_2 cannot remain constant as x_1 varies. Nevertheless, we eliminate the Λ length in favor of the link, and obtain

$$P'_k(x_1, x_3; \lambda_1, \lambda_2) = f'_k(\lambda_1, \lambda_2)\,(\lambda_1\lambda_2/\eta_{1k}\eta_{2k}\mu_2) \times \exp(-g_{1k}x_1 - g_{3k}x_3), \tag{A.3}$$

where $g_{1k} = \lambda_1/\eta_{1k} - \lambda_2\mu_1/\eta_{2k}\mu_2$, $g_{3k} = \lambda_2/\eta_{2k}\mu_2$, and

$$f'^{-1}_k(\lambda_1, \lambda_2) = (\lambda_1\lambda_2/\eta_{1k}\eta_{2k}\mu_2) \int_0^{B_{3k}} dx_3 \int_0^{x_3} dx_1 \exp(-g_{1k}x_1 - g_{3k}x_3). \tag{A.4}$$

The new Jacobian factor μ_2 is included in (A.3), and P'_k is normalized over the range of the true Ξ^0 and link lengths. The Ξ^0 length cannot exceed the length of the link, because $\theta \leq 90$ deg at our momenta.

Finally, we assume that the lengths of the Ξ^0 and the link, x_1 and x_3, have been measured to be ℓ_{1k} and ℓ_{3k} with uncertainties σ_{1k} and σ_{3k}, respectively. We take the measurements to be normally distributed about the true values and fold Gaussian error functions into the probability function in (A.3). The probability for this pair of measurements is

$$P^Q_k(\ell_{1k}, \ell_{3k}; \lambda_1, \lambda_2) = \int_0^{B_{3k}} dx_3 Q_{3k}(x_3, \ell_{3k}) \int_0^{x_3} dx_1 Q_{1k}(x_1, \ell_{1k}) \times P'_k(x_1, x_3; \lambda_1, \lambda_2). \tag{A.5}$$

The Gaussian functions Q_{1k} and Q_{3k} are normalized over the range of allowed measurements; the normalization constant depends on the true length for any finite measurement range, modifying the Gaussian form. The uncertainty in the measured link is small relative to 0.5 cm, its minimum value; therefore, $Q_{3k}(x_3, \ell_{3k})$ approximates a δ function, and

we obtain

$$P_k^{Q'}(\ell_{1k}, \ell_{3k}; \lambda_1, \lambda_2) = \int_0^{\ell_{3k}} dx_1 Q_{1k}(x_1, \ell_{1k}) P_k'(x_1, \ell_{3k}; \lambda_1, \lambda_2), \tag{A.6}$$

$$Q_{1k}(x_1, \ell_{1k}) = C_{1k}(x_1)(1/\sqrt{2\pi}\,\sigma_{1k}) \exp[-(x_1-\ell_{1k})^2/2\sigma_{1k}^2], \tag{A.7}$$

and

$$C_{1k}^{-1}(x_1) = (1/\sqrt{2\pi}\,\sigma_{1k}) \int_{a_{1k}}^{b_{1k}} d\ell \, \exp[-(x_1-\ell)^2/2\sigma_{1k}^2]. \tag{A.8}$$

The combined likelihood for N events, when the links are accurately measured, is

$$\mathcal{L}^Q(\lambda_1, \lambda_2) = \prod_{k=1}^{N} P_k^{Q'}(\ell_{1k}, \ell_{3k}; \lambda_1, \lambda_2). \tag{A.9}$$

We use this likelihood function for the lifetime analysis.

2. <u>Lifetime from the Link Joining the Ξ^0 Production and Λ Decay Vertices</u>

For collinear Ξ^0 decays, we rewrite (A.1) in terms of the sum, $x_3 = x_1 + x_2$, and the difference, $z = x_1 - x_2$, of the fermion lengths, then we integrate over the difference, $-x_3 \leq z \leq x_3$. The link is accurately measured; we take $x_3 = \ell_{3k}$ and obtain

$$P_k^X(\ell_{3k}; \lambda_1, \lambda_2) = f_k^X(\lambda_1, \lambda_2)\left(\frac{\lambda_1\lambda_2}{\lambda_2\eta_{1k}-\lambda_1\eta_{2k}}\right)$$

$$\times [\exp(-\lambda_1\ell_{3k}/\eta_{1k}) - \exp(-\lambda_2\ell_{3k}/\eta_{2k})], \tag{A.10}$$

or, when $\lambda_1/\eta_{1k} = \lambda_2/\eta_{2k}$,

$$P_k^{X'}(\ell_{3k}; \lambda_1, \lambda_2) = f_k^{X'}(\lambda_1, \lambda_2)(\lambda_1\lambda_2/\eta_{1k}\eta_{2k}) \quad \ell_{3k}\exp(-\lambda_1\ell_{3k}/\eta_{1k}). \tag{A.10'}$$

0 0 0 0 0 2 2 3 2 0 0 2 3 2 8 6 3

The normalization is over the measurement range, $0.5 \text{ cm} \leq \ell_{3k} \leq b_{3k}$. Here the combined likelihood for N events is

$$\mathcal{L}^X(\lambda_1, \lambda_2) = \prod_{k=1}^{N} P_k^X(\ell_{3k}; \lambda_1, \lambda_2). \qquad (A.11)$$

FOOTNOTES AND REFERENCES

1. R. Armenteros, K. H. Barker, C. C. Butler, A. Cachon, and C. M. York, Philos. Mag. 43, 597 (1952); E. W. Cowan, C. D. Anderson, R. B. Leighton, and V. A. J. Van Lint, Phys. Rev. 92, 1089 (1953); R. Armenteros, B. Gregory, A. Lagarrigue, L. Leprince-Ringuet, F. Muller, and C. Peyrou, Nuovo Cimento Suppl. (9) 12, 327 (1954).
2. M. Gell-Mann, Nuovo Cimento Suppl. (10) 4, 848 (1956); Kazuhiko Nishijima, Progr. Theoret. Phys. (Kyoto) 13, 285 (1955).
3. L. W. Alvarez, P. Eberhard, M. L. Good, W. Graziano, H. K. Ticho, and S. G. Wojcicki, Phys. Rev. Letters 2, 215 (1959).
4. J. P. Berge, P. Eberhard, J. R. Hubbard, D. W. Merrill, J. B. Shafer, F. T. Solmitz, and M. L. Stevenson, "Some Properties of Ξ^- and Ξ^0 Hyperons Produced in K^-p Interactions Between 1.05 and 1.7 BeV/c," to be published in Phys. Rev.
5. M. L. Stevenson, J. P. Berge, J. R. Hubbard, G. R. Kalbfleisch, J. B. Shafer, F. T. Solmitz, S. G. Wojcicki, and P. G. Wohlmut, Phys. Letters 9, 349 (1964).
6. J. R. Hubbard, J. P. Berge, G. R. Kalbfleisch, J. B. Shafer, F. T. Solmitz, M. L. Stevenson, S. G. Wojcicki, and P. G. Wohlmut, Phys. Rev. 135, B183 (1964).
7. M. Ferro-Luzzi, M. H. Alston, A. H. Rosenfeld, and S. G. Wojcicki, Phys. Rev. 130, 1568 (1963).
8. M. Gell-Mann and A. Pais, Proceedings of the 1954 Glasgow Conference on Nuclear and Meson Physics, p. 342 (Pergamon Press Ltd., London, 1955). For a recent review, see N. P. Samios, Proceedings of the International Conference on Weak Interactions, 1965 (Argonne National Laboratory, 1965), p. 189.
9. Joseph J. Murray, Lawrence Radiation Laboratory Report UCRL-9506, 1960 (unpublished).
10. D. H. Stork, H. K. Ticho, J. R. Hubbard, D. O. Huwe, G. R. Kalbfleisch, J. Kirz, D. H. Miller, and C. G. Wohl, Lawrence Radiation Laboratory, private communication.

0 0 0 0 0 2 2 3 2 0 0 5 2 5 2 8 7 4

11. M. A. Alston, F. T. Solmitz, J. Kronenthal, G. Hashiguchi, and J. Neufeld, Alvarez Physics Note 422, Lawrence Radiation Laboratory, 1962 (unpublished).

12. B. Pardoe, Alvarez Physics Note 398, Lawrence Radiation Laboratory, 1962 (unpublished).

13. The threshold for $K^- p \rightarrow \Lambda K^0 \bar{K}^0$ is 1.7 BeV/c, the high-energy limit of this experiment.

14. Joseph Adam Schwartz (Ph. D. Thesis), Lawrence Radiation Laboratory Report UCRL-11360, 1965 (unpublished). A smooth curve was drawn through the compilation presented.

15. Darrell O. Huwe (Ph. D. Thesis), Lawrence Radiation Laboratory Report UCRL-11291, 1964 (unpublished).

16. S. G. Wojcicki, Phys. Rev. 135, B484 (1964); S. G. Wojcicki, M. H. Alston, and G. R. Kalbfleisch, Phys. Rev. 135, B495 (1964).

17. Ten of the 52 $\Xi^0 K^+ \pi^-$ events were identified at an early stage because of obvious K^+ decays.

18. J. Richard Hubbard, Alvarez Physics Note 496, Lawrence Radiation Laboratory, 1964 (unpublished).

19. A. H. Rosenfeld, A. Barbaro-Galtieri, W. H. Barkas, P. L. Bastien, J. Kirz, and M. Roos, Rev. Mod. Phys. 37, 633 (1965).

20. V. Cook, Bruce Cork, T. F. Hoang, D. Keefe, L. T. Kerth, W. A. Wenzel, and T. F. Zipf, Phys. Rev. 123, 320 (1961).

21. A. N. Diddens, E. W. Jenkins, T. F. Kycia, and K. F. Riley, Phys. Rev. Letters 10, 262 (1963).

22. The discussion of crossing matrices is based on that of D. Amati, L. L. Foldy, A. Stanghellini, and L. Van Hove, Nuovo Cimento (10) 32, 1685 (1964). See also Andrzej Kotański and Kacper Zalewski, Acta Phys. Polon. (Warsaw) 26, 117 (1964).

23. See M. E. Rose, Elementary Theory of Angular Momentum (John Wiley and Sons, Inc., New York, 1957).

24. A. Ramakrishnan, R. Thunga, T. K. Radha, G. Bhamathi, and S. Indumathi, Nucl. Phys. 37, 585 (1962).

25. M. Ferro-Luzzi, R. George, Y. Goldschmidt-Clermont, V. P. Henri, B. Jongejans, D. W. G. Leith, G. R. Lynch,

F. Muller, and J. M. Perreau, Phys. Letters 17, 155 (1965).

26. R. C. King, Nuovo Cimento (10) 30, 1220 (1963).

27. M. E. Ebel and P. B. James, Phys. Rev. Letters 15, 805 (1965). These authors ignore crossing symmetry and include $Y_1^*(1385)$ in the u channel, but not in the s channel.

28. A. W. Martin and K. C. Wali, Phys. Rev. 130, 2455 (1963).

29. K. Gottfried and J. D. Jackson, Nuovo Cimento (10) 34, 735 (1964); L. Durand, III, and Y. T. Chiu, Phys. Rev. 139, B646 (1965).

30. F. Gürsey, A. Pais, and L. A. Radicati, Phys. Rev. Letters 13, 299 (1964); S. P. Rosen and S. Pakvasa, Phys. Rev. Letters 13, 773 (1964).

31. W. Willis, H. Courant, H. Filthuth, P. Franzini, A. Minguzzi-Ranzi, A. Segar, R. Engelmann, V. Hepp, E. Kluge, R. A. Burnstein, T. B. Day, R. G. Glasser, A. J. Herz, B. Kehoe, B. Sechi-Zorn, N. Seeman, and G. A. Snow, Phys. Rev. Letters 13, 291 (1964). Their first solution gives f = 0.37 with 45% probability, and their second solution gives f = 0.64 with 17% probability.

32. C. G. Wohl, F. T. Solmitz, and M. L. Stevenson, Bull. Am. Phys. Soc. II 10, 529 (1965); Charles Gordon Wohl (Ph. D. Thesis), Lawrence Radiation Laboratory Report UCRL-16288, 1965 (unpublished); M. L. Stevenson, Bull. Am. Phys. Soc. II 10, 1179 (1965).

33. C. A. Levinson, H. J. Lipkin, and S. Meshkov, Phys. Letters 1, 44 (1962).

34. S. Meshkov, G. A. Snow, and G. B. Yodh, Phys. Rev. Letters 12, 87 (1964).

35. M. B. Watson, M. Ferro-Luzzi, and R. D. Tripp, Phys. Rev. 131, 2248 (1963).

36. P. L. Bastien and J. P. Berge, Phys. Rev. Letters 10, 188 (1963).

37. Angela Barbaro-Galtieri (Lawrence Radiation Laboratory), private communication, 1966.

38. V. Barger and M. H. Rubin, Phys. Rev. Letters 14, 713 (1965); J. C. Carter, J. J. Coyne, and S. Meshkov, Phys. Rev. Letters 14, 523 (1965).

0 00 00 00 02 23 20 03 26 62 88 5

39. J. C. Carter, J. J. Coyne, S. Meshkov, D. Horn, M. Kugler, and H. J. Lipkin, Phys. Rev. Letters 15, 373 and 768 (1965).

40. J. D. Jackson, Phys. Rev. Letters 15, 990 (1965).

41. M. Ademollo and R. Gatto, Nuovo Cimento (10) 30, 429 (1963).

42. Frank S. Crawford, Jr., Proceedings of the International School of Physics "Enrico Fermi", Course XXVI (Academic Press, New York, 1963), p. 88.

43. W. Shakespeare, Julius Caesar, Act V, Scene 3, lines 67-69 in The Complete Works of Shakespeare, Hardin Craig, Ed. (Scott, Foresman, and Co., Chicago, 1961), p. 795.

44. L. Jauneau, D. Morellet, U. Nguyen Khac, P. Petiau, A. Rousset, H. H. Bingham, D. C. Cundy, W. Koch, M. Nikolic, B. Ronne, O. Skjeggestad, H. Sletten, F. W. Bullock, A. K. Common, M. J. Esten, C. Henderson, F. R. Stannard, J. M. Scarr, J. Sparrow, A. G. Wilson, A. Halsteinslid, and R. Möllerud, Proceedings of the Sienna International Conference on Elementary Particles (Societa Italiana di Fisica, Bologna, 1963), Vol. 1, p. 1.

45. D. D. Carmony, G. M. Pjerrou, P. E. Schlein, W. E. Slater, D. H. Stork, and H. K. Ticho, Phys. Rev. Letters 12, 482 (1964).

46. R. H. Dalitz, Proc. Phys. Soc. (London) A64, 667 (1951).

47. N. P. Samios, Phys. Rev. 121, 275 (1961).

48. Margaret Alston and Frank T. Solmitz did most of the Dalitz event analysis.

49. G. B. Cvijanovich, E. A. Jeannet, and E. C. G. Sudarshan, Phys. Rev. Letters 14, 117 (1965).

50. J. H. Christenson, J. W. Cronin, V. L. Fitch, and R. Turlay, Phys. Rev. Letters 13, 138 (1964).

51. G. Rinaudo, A. Marzari-Chiesa, G. Gidal, and A. E. Werbrouck, Phys. Rev. Letters 14, 761 (1965).

52. C. N. Yang, Phys. Rev. 77, 242 (1950).

53. D. W. Joseph, Nuovo Cimento (10) 16, 997 (1960).

54. A discussion on this topic with Dr. Henry P. Stapp (Lawrence Radiation Laboratory) was very helpful.

55. R. P. Feynman and M. Gell-Mann, Phys. Rev. 109, 193 (1958).

56. Nicola Cabibbo, Phys. Rev. Letters 10, 531 (1963).

57. Murray Gell-Mann, Physics 1, 63 (1964).

58. R. F. Dashen and M. Gell-Mann, Phys. Letters 17, 145 (1965); Benjamin W. Lee, Phys. Rev. Letters 14, 676 (1965).

59. S. Fubini and G. Furlan, Physics 1, 229 (1965); Stephen L. Adler, Phys. Rev. Letters 14, 1051 (1965); William I. Weisberger, Phys. Rev. Letters 14, 1047 (1965); D. Amati, C. Bouchiat, and J. Nuyts, Phys. Letters 19, 59 (1965); C. A. Levinson and I. J. Muzinich, Phys. Rev. Letters 15, 715 (1965); R. Gatto, L. Maiani, and G. Preparata, Phys. Rev. Letters 16, 377 (1966).

60. R. H. Good, R. P. Matsen, F. Muller, O. Piccioni, W. M. Powell, H. S. White, W. B. Fowler, and R. W. Birge, Phys. Rev. 124, 1223 (1961).

61. L. Okun' and B. Pontecorvo, Zh. Eksperim. i Teor. Fiz. 32, 1587 (1957) [English transl.: Soviet Phys. - JETP 5, 1297 (1957)].

62. L. Wolfenstein, Phys. Rev. Letters 13, 562 (1964); T. D. Lee and L. Wolfenstein, Phys. Rev. 138, B1490 (1965).

63. R. E. Behrends and A. Sirlin, Phys. Rev. 121, 324 (1961).

64. T. D. Lee, Phys. Rev. Letters 9, 319 (1962).

65. A. Barbaro-Galtieri, W. H. Barkas, H. H. Heckman, J. W. Patrick, and F. M. Smith, Phys. Rev. Letters 9, 26 (1962).

66. U. Nauenberg, P. Schmidt, J. Steinberger, S. Marateck, R. J. Plano, H. Blumenfeld, and L. Seidlitz, Phys. Rev. Letters 12, 679 (1964).

67. B. d'Espagnat, Nuovo Cimento (10) 18, 287 (1960); L. Wolfenstein, Nuovo Cimento (10) 29, 859 (1963).

68. Sheldon Lee Glashow, Phys. Rev. Letters 6, 196 (1961).

69. R. E. Behrends and A. Sirlin, Phys. Rev. Letters 8, 221 (1962).

70. L. B. Okun', Yadern. Fiz. 1, 1132 (1965) [English transl.: Soviet J. Nucl. Phys. 1, 806 (1965)].

71. E. Fermi, Z. Physik 88, 161 (1934); V. P. Belov, B. S. Mingalev, and V. M. Shekhter, Zh. Eksperim. i Teor. Fiz. 38, 541 (1960) [English transl.: Soviet Phys. - JETP 11, 392 (1960)].

72. D. D. Carmony and G. M. Pjerrou, Phys. Rev. Letters 10, 381 (1963).

73. G. W. London, R. R. Rau, N. P. Samios, S. S. Yamamoto, M. Goldberg, S. Lichtman, M. Primer, and J. Leitner, Phys. Rev. 143, 1034 (1966).

0 00 00 00 02 23 20 05 26 63 80 7

This report was prepared as an account of Government sponsored work. Neither the United States, nor the Commission, nor any person acting on behalf of the Commission:

A. Makes any warranty or representation, expressed or implied, with respect to the accuracy, completeness, or usefulness of the information contained in this report, or that the use of any information, apparatus, method, or process disclosed in this report may not infringe privately owned rights; or

B. Assumes any liabilities with respect to the use of, or for damages resulting from the use of any information, apparatus, method, or process disclosed in this report.

As used in the above, "person acting on behalf of the Commission" includes any employee or contractor of the Commission, or employee of such contractor, to the extent that such employee or contractor of the Commission, or employee of such contractor prepares, disseminates, or provides access to, any information pursuant to his employment or contract with the Commission, or his employment with such contractor.